

GENETICALLY ENGINEERED SENSORS OF CELL SIGNALING

Thesis by

Micah Seth Siegel

In Partial Fulfillment of the Requirements

for the Degree of

Doctor of Philosophy

California Institute of Technology

Pasadena, California

2000

(Submitted December 16, 1999)

© 1999

Micah Seth Siegel

All rights reserved

Acknowledgement

This project began at Caltech, where I was a graduate student in the Computation and Neural Systems program. It was completed at the University of California, Berkeley, where I was a visiting scholar in the department of Molecular and Cellular Biology. The project would have been unsuccessful without the intellectual stimulation and practical advice provided by colleagues at these institutions.

During my first two years at Caltech, I was a student in Carver Mead's laboratory and designed analog VLSI circuits. Carver inspired me with clear and gentle explanations of the physics of computation. He influenced this thesis in subtle ways. Soon after joining Carver's laboratory I became intrigued by the possibility that techniques from molecular biology could be used to create tools for biology. I am grateful to Carver for encouraging me to pursue these interests.

Henry Lester provided a home for me during my initial work in molecular biology. Scott Fraser inspired me with his technical creativity, helped me to define this project and helped me to arrange my collaboration with U.C. Berkeley.

I am grateful to my doctoral thesis committee at Caltech: Scott Fraser, Udi Isacoff (U.C. Berkeley), Gilles Laurent, Henry Lester and Carver Mead. This committee allowed me the independence to pursue a project that appeared to be quixotic and outside of my ken. Each of these members gave invaluable advice at different times; additionally, I was buoyed by their concern for my scientific and personal well-being.

At Caltech and at U.C. Berkeley, many colleagues provided invaluable discussion about molecular biology and electrical engineering. Some of these friends include Shane Atwell, Tine Bak, Alison Barth, Grischa Chandy, Joe Dynes, Sarah Farivar, Jennifer Linden, Sanjoy Mahajan, Anna Penn, Pam Reinagel, David Specca, and Emily Transue.

Sanjoy Mahajan and Carver Mead at Caltech gave valuable advice concerning the physical limits of signal detection. Sanjoy Mahajan taught me to estimate physical quantities based on order-of-magnitude calculations, a skill that I have found useful in a variety of non-scientific projects, including a technology startup. Norman Davidson at Caltech shared advice on the physical chemistry of GFP. Tom Alber at U.C.

Berkeley shared crystal coordinates for the green fluorescent protein and provided advice on circular permutations of this protein.

I thank the members of Ehud Isacoff's laboratory at U.C. Berkeley for providing valuable discussions about ion channels and teaching me various techniques related to cellular imaging, oocyte physiology, and RNA injection. In particular, I benefited from many challenging and lively discussions with Lidia Mannuzzu and Karen Zito.

Much of the work in chapters three and four was completed in collaboration with Sarah Farivar, an undergraduate -- and subsequently a technician -- in the Isacoff laboratory. The work in chapter five was completed in collaboration with Giovanna Guerrero, Botond Roska, Rick Harris, and Sheffa Gordon. I was privileged to mentor Giovanna Guerrero, Sheffa Gordon, and Botond Roska during their rotation projects in the Isacoff laboratory.

Larry Salkoff at Washington University discovered that FlaSh expression levels could be greatly improved by removing a spurious 5' ATG in the un-translated region of the Shaker gene. Rafa Yuste and Marty Chalfie at Columbia University gave invaluable advice on GFP expression in mammalian systems.

This research was completed while I was supported by a pre-doctoral fellowship from the Howard Hughes Medical Institute. I am grateful to HHMI for the freedom afforded by their fellowship, and for the credibility their organization brought to this work in its initial stages. I was also supported by and honored to receive the Milton Mohr fellowship at Caltech.

My thanks to Claire Berkman and to Marvin Siegel for generously collaborating on a difficult project that eventually led to this thesis.

Finally, my deepest thanks are due to Udi Isacoff, my collaborator and host at U.C. Berkeley. Udi graciously allowed me to pursue this project in his laboratory and provided patient encouragement during its completion. Udi's intellectual contribution is embedded in this work; he has become a mentor and a friend in many ways.

Abstract

Measuring electrical activity in large numbers of cells with high spatial and temporal resolution is a fundamental problem for the study of neural development and information processing. To address this problem, we have constructed FlaSh: a novel, genetically-encoded probe that can be used to measure transmembrane voltage in single cells. We fused a modified green fluorescent protein (GFP) into a voltage-sensitive potassium channel so that voltage dependent rearrangements in the potassium channel induce changes in the fluorescence of GFP. A voltage sensor encoded into DNA has the advantage that it may be introduced into an organism non-invasively and targeted to specific developmental stages, brain regions, cell types, and sub-cellular compartments.

We also describe modifications to FlaSh that shift its color, kinetics, and dynamic range. We used multiple green fluorescent proteins to produce variants of the FlaSh sensor that generate ratiometric signal output via fluorescence resonance energy transfer (FRET). Finally, we describe initial work toward FlaSh variants that are sensitive to G-protein coupled receptor (GPCR) activation. These sensors can be used to design functional assays for receptor activation in living cells.

Table of Contents

CHAPTER 1

Introduction

- 1.1 Overview 9
- 1.2 Genetic probes 10

CHAPTER 2

FlaSh: A genetically encoded optical probe of membrane voltage

- 2.1 Introduction 15
- 2.2 Results 16
- 2.3 Discussion 19
- 2.4 Conclusion 24

CHAPTER 3

Modifications to FlaSh

- 3.1 Tandem FlaSh constructs 29
- 3.2 FlaSh response to retinal voltage traces 32
- 3.3 Voltage-shifted FlaSh 34
- 3.4 Fast FlaSh: FlaSh-IR 37
- 3.5 Slow FlaSh 38

GFP inserted into Shaker at various locations

- 3.6 A review of methods 40
- 3.7 Chimeric proteins between GFP and Shaker K⁺ channel 49

CHAPTER 4

FlaSh with altered spectra: eCFP, eYFP, eGFP-FlaSh

- 4.1 A review of fluorescent proteins 55
- 4.2 Structure of GFP and improvements 55
- 4.3 Altering the spectrum of GFP 58
- 4.4 Useful GFP variants for FRET: eYFP, eCFP, eGFP 61
- 4.5 FlaSh color variants 64

Applications of FlaSh color variants

- 4.6 FlaSh sensors based on FRET 72
- 4.7 eYFP/eCFP Shaker chimeric proteins 72
- 4.8 Summary 77

CHAPTER 5

G protein-coupled FlaSh

5.1	GPCRs as therapeutic targets	78
5.2	Inwardly rectifying potassium channels	81
5.3	GFP insertion locations in Girk3.1	81
5.4	eYFP/eCFP-Girk3.1	84
5.5	Summary	85

CHAPTER 6

Future directions

6.1	Techniques for random optimization	86
6.2	Evolutionary PCR	87
6.3	Conclusion	89

APPENDICES 91

REFERENCES 94

For MB

“We shall not cease from exploration
And the end of all our exploring
Will be to arrive where we started
And know the place for the first time.”
-T.S. Eliot (1934)

Chapter 1. Introduction

1.1 Overview

How does one image the brain? This thesis began with the challenge of visualizing electrical activity in living tissue. The fundamental difficulty is that cells can be small ($<5 \mu\text{m}$), and action potentials can be short ($<5 \text{ msec}$). For example, it is estimated that $1 \mu\text{l}$ of cerebral cortex contains one million (1,000,000) neurons and one billion (1,000,000,000) synapses.

Traditionally, one tried to solve this problem by staining the tissue with a probe from the outside or by inserting electrodes into the tissue. In this thesis, we describe a different approach to the problem of imaging living tissue. We ask the question: how can one induce the tissue to synthesize a probe from the inside? This approach requires us to design a novel gene whose protein product, when expressed in living tissue, produces a functional fluorescent sensor. The desired properties of this sensor are: first, to measure individual action potentials; and second, to relay information about these action potentials via a fluorescence change.

As described in chapter 2, nature has solved both of these problems for us. To measure individual action potentials, we exploit the Shaker potassium channel, which has been designed by nature to measure and to respond to individual action potentials. To create a fluorescence readout, we exploit the green fluorescent protein (GFP), which is a fluorescent protein found in the jellyfish *Aequorea victoria*. We have combined the genes for these two proteins to create a functional genetic sensor called FlaSh. FlaSh produces a fluorescent signal that is triggered by individual electrical events in living cells.

In chapter 3, we describe various precursors to FlaSh. For example, we enumerate some chimeric proteins that did not produce functional sensors. We also describe modifications to FlaSh that change its color, its kinetics, and improve its dynamic range.

In chapter 4, we describe various attempts to improve FlaSh by using fluorescence resonance energy transfer, which is a physical effect whereby two fluorescent molecules can interact in a manner that is dependent on their distance and their mutual orientation. We describe sensors that contain multiple copies of GFP and that produce a ratiometric fluorescence output. In principle, these sensors have the advantage that they can be improved by rational or semi-rational genetic manipulations.

In chapter 5, we discuss initial work toward a more generalized sensor of cellular activity. In particular, we describe ratiometric fluorescent sensors designed to respond to G-protein coupled receptor (GPCR) activation. When successful, these sensors will have unique commercial applications in the area of high-throughput drug screening.

Finally, in chapter 6, we summarize future directions for this work. The field of genetically encoded physiological sensors is subtle and largely unexplored. The initial efforts described in this thesis will have been most successful if we can inspire others to improve on their design and to use them in living tissue.

1.2 Genetic Probes

[Adapted from Siegel, M.S.: Genetic Probes: New ways to watch cells in action. *Current Biology*, 1997 Sep 1, 7(9).]

Introduction

In many areas of biology, it would be highly useful to be able to record the activity of multiple, individual living cells, ideally in their natural context. Some progress towards this goal has been made with the development of fluorescent indicator dyes, which have revolutionized our understanding of cellular physiology by allowing continuous measurements of activities in living cells. At present, these dyes must be synthesized *in vitro* and introduced into cells by microinjection or as permeant esters. In many cases, it would be a significant advantage to be able to deliver the indicator dye to a specific cell population, but achieving this in general is a difficult problem. An elegant approach to this problem would be to encode protein-based sensors in DNA; in principle, such a protein-based sensor could be targeted *in vivo* by using gene transfer or some other molecular genetic approach. Several recent papers describe initial steps towards the development of optically active proteins that can detect or perturb cellular activity.

A protein-based sensor should have some means of emitting light, through either luminescence or fluorescence. Miesenböck and Rothman (Miesenböck and Rothman 1997) have exploited the light-emitting enzyme, *Cypridina* luciferase, to measure synaptic vesicle exocytosis in cultured cells. Synaptic vesicle exocytosis is a key event in the transmission of signals between neurons, so in principle a way of following the process in living cells could be used to monitor activity in a neural circuit. The core of the

Miesenbock and Rothman sensor, *Cypridina* luciferase, is a member of a diverse class of enzymes that emit light in the presence of molecular oxygen and their substrate, luciferin. In the past twelve years, the genes for several luciferases have been cloned and expressed in mammalian cells, and in the case of firefly luciferase the protein has been crystallized and its structure determined by X-ray diffraction (Conti, Franks et al. 1996). To make a sensor protein for monitoring synaptic vesicle exocytosis, Miesenbock and Rothman (Miesenböck and Rothman 1997) constructed fusion proteins, dubbed 'synaptolucins', in which *Cypridina* luciferase was linked to proteins known to be associated with the synaptic vesicle – synaptotagmin and VAMP-2/synaptobrevin.

These synaptolucin fusion proteins lock the luciferase enzyme into the lumen of the synaptic vesicle. Luciferase requires its substrate to generate light, and this was loaded into the extracellular medium, where the substrate is largely inaccessible to the intracellular luciferase (but see below). The idea is that, when the vesicle fuses with the presynaptic membrane, luciferase is exposed to its substrate, catalyzing the emission of a stream of photons until the vesicle is re-internalized. Miesenbock and Rothman (Miesenböck and Rothman 1997) infected cultured hippocampal neurons with a herpes virus vector carrying the gene for the synaptolucin fusion protein. When the infected cells were depolarized with a high potassium solution, Miesenbock and Rothman (Miesenböck and Rothman 1997) were able to record the light emitted by the activated synaptolucin and thus measure time-averaged synaptic activity levels.

Problems with genetic probes based on Luciferase

Unfortunately, Miesenbock and Rothman (Miesenböck and Rothman 1997) were not able to visualize individual vesicle fusion events. The sensitivity of the synaptolucin system is undermined somewhat by the permeability of cell membranes to the luciferin substrate. At saturating luciferin concentrations, vesicle fusion was not required for light emission, indicating that luciferin can diffuse into synaptic vesicles. This forced Miesenbock and Rothman (Miesenböck and Rothman 1997) to reduce the luciferin concentration to approximately 3% of its saturating concentration. Engineering a luciferin substrate with a cleaner membrane partition, or a luciferase enzyme with greater affinity for its substrate, should recover at least an order of magnitude in signal strength; at saturating luciferin concentrations, photon emissions would be expected to increase about 35-fold. With greater signal size, it may be possible

to detect individual vesicle fusion events in culture, and perhaps eventually to visualize averaged synaptic activity *in vivo*.

Peeking at cells with other luminescent proteins

Other luminescent proteins have been retooled into physiological indicators. Aequorin is a calcium-sensitive photoprotein consisting of an apoprotein and a prosthetic group, coelenterazine. Rizzuto *et al.* (Rizzuto, Simpson *et al.* 1992) expressed recombinant aequorin in mammalian cells to measure calcium concentrations within the mitochondria. They directed the sensor to the sub-cellular organelle by attaching a targeting pre-sequence to the aequorin apoprotein, and reconstituted functional aequorin by incubating the cells in the presence of coelenterazine. When the agonist was applied to the aequorin-expressing cells, calcium transients were induced in their mitochondria which could be visualized as the photoproteins discharged. Targeted aequorin has since been used by Rizzuto and others to measure calcium concentrations in the nucleus, the sarcoplasmic reticulum and the cytoplasmic rim just beneath the plasma membrane.

Genetic probes based on green fluorescent protein (GFP)

Both the luciferase and aequorin systems require substrates or cofactors to generate light. For example, Rizzuto *et al.* (Rizzuto, Simpson *et al.* 1992) had to incubate their transfected cells overnight in the presence of coelenterazine to charge the photoproteins, and photoemission slowly discharged the sensor population. A further drawback of these systems is that, relative to fluorescence, chemiluminescence generates very few photons and so can be difficult to image at high spatial or temporal resolution. An alternative approach is to re-engineer a naturally fluorescent protein, such as the green fluorescence protein (GFP) from *Aequorea victoria*. GFP has been widely used as a marker for gene expression (Chalfie, Tu *et al.* 1994) and can be targeted to specific classes of cells or sub-cellular organelles (Rizzuto, Brini *et al.* 1996). The crystal structure of GFP has recently been solved (Ormö, Cubitt *et al.* 1996; Yang, Moss *et al.* 1996). Although naturally occurring GFP is rather insensitive to environmental variations, aided by

knowledge of its three-dimensional structure, it is possible to engineer environmentally sensitive GFP variants for use as protein sensors. (For example, see chapter six.)

The few available GFP-based sensors exploit resonance energy transfer (Stryer 1978) (see chapter four) between GFP variants of different colours. Resonance energy transfer is a process whereby, given appropriate excitation/emission spectra, one fluorescent molecule can be excited indirectly *via* a second fluorescent molecule. This effect depends strongly on the distance between two fluorescent molecules and their relative orientation. As a consequence, resonance energy transfer can be used to amplify small steric changes within a protein into large changes in fluorescence. Thus, Heim and Tsien (Heim and Tsien 1996) and Mitra *et al.* (Mitra, Silva *et al.* 1996) have used GFP to monitor protease activity *in vitro*. Both groups engineered protease consensus sequences into a synthetic linker connecting two GFP variants. Proteolytic cleavage at the consensus sequence disrupted energy transfer between the molecules, so that the proteolysis reaction can be monitored directly.

Romoser *et al.* (Romoser, Hinkle *et al.* 1997) used the same technique to design a calcium-calmodulin-dependent fluorescent sensor. They engineered a calmodulin-binding sequence into the linker between two GFP variants; binding of calmodulin to the engineered fusion protein, which is dependent of calcium concentration, reduced energy transfer between the two GFPs. Romoser *et al.* (Romoser, Hinkle *et al.* 1997) used this sensor to monitor cytosolic free calcium concentration by microinjecting the protein sensor along with calmodulin into mammalian cells. Ultimately, one would want to introduce the sensor genetically, and significant improvements in the sensor design should make this possible.

Poking at cells with genetic probes

Optically-active proteins can also be used to manipulate cellular physiology with light. Nirenberg and Cepko (Nirenberg and Cepko 1993) devised a clever cell-ablation technique to lesion specific classes of cells from a neural circuit. Their general approach is to engineer the target cells to express the gene for the enzyme β -galactosidase. To ablate the target cells, a fluorogenic, membrane-permeant β -galactosidase substrate is added to the tissue. Those cells expression β -galactosidase cleave the substrate, unveiling its fluorescent moiety. Once labeled, the dye-filled cells can be killed by photodynamic damage. Using the

technique, Nirenberg and Cepko (Nirenberg and Cepko 1993) have ablated subclasses of amacrine cells in the retina, neurons in mouse cerebral cortex, rod photoreceptors and developing zebrafish embryos. One significant advantage of the technique is that β -galactosidase is a widely used reporter enzyme, so large numbers of mice and invertebrate strains are already available that selectively express β -galactosidase in specific classes of cells.

Conclusion

Genetically encoded sensors can be introduced into cells or organisms by DNA transfer techniques, including viral vectors or ballistic methods. Eventually, sensors will be delivered directly into transgenic animals, which could redefine the research tools used to make measurements from cellular ensembles. The central advantage of a genetically-encoded probe is that it can be targeted *in vivo* using molecular biology. Targeting sequences and fusion proteins can be used to direct probes to specific sub-cellular organelles. Promoter sequences can be used to direct the expression of neural probes to specific times during development, specific types of neurons or specific brain regions. The possibilities here are subtle and largely unexplored.

Chapter 2

A genetically encoded optical probe of membrane voltage.

[Adapted from Siegel, M.S. and Isacoff E.Y.: A genetically encoded optical probe of membrane voltage. *Neuron*, 1997 Oct, 19(4), p. 734-41.]

2.1 Introduction

Fluorescent indicators have revolutionized our understanding of cellular physiology by providing continuous measurements in single cells and cell populations. Presently, these dyes must be synthesized chemically and introduced as hydrolyzable esters or by microinjection (Cohen and Leshner 1986; Gross and Loew 1989; Tsien 1989). Delivering indicator dyes to specific cell populations could be significant advantage for many experiments, but this has proven to be a difficult problem. In the absence of such localization, optical measurements in neural tissue usually cannot distinguish whether a signal originates from electrical activity in neurons or glia, nor which types of neurons are involved. One general approach to this problem is to encode protein-based sensors into DNA. This permits the sensor to be placed under the control of cell-specific promoters and to be introduced in vivo or in vitro using gene transfer techniques.

A protein-based optical sensor must have some means of emitting light. Our approach was to exploit the green fluorescent protein (GFP) cloned from the jellyfish *Aequorea victoria* (Prasher, Eckenrode et al. 1992). GFP is a small protein (238 amino acids). Its chromophore is generated autocatalytically (Heim and Tsien 1996), and the protein is stable and functional in many cell types. The crystal structure of GFP has been solved by X-ray diffraction (Ormö, Cubitt et al. 1996; Yang, Moss et al. 1996), and mutations have been found that alter its spectral properties (Heim and Tsien 1996), providing some guidance as to how GFP might be modified for new applications. Several recent studies have used GFP to mark gene expression and to trace individual proteins in a wide variety of organisms (Chalfie, Tu et al. 1994; Amsterdam, Lin et al. 1995; Marshall, Molloy et al. 1995).

This thesis describes a novel GFP-based sensor that we have designed to measure fast membrane potential changes in single cells and in populations of cells. The naturally occurring GFP, a stable cytoplasmic protein, is not sensitive to the voltage across the plasma membrane. Therefore, we fused GFP to the voltage-activated Shaker K⁺ channel (Tempel, Papazian et al. 1987; Baumann, Grupe et al. 1988;

Kamb, Tseng-Crank et al. 1988). Our idea was that the voltage-dependent rearrangements in the channel could be transmitted to GFP, resulting in a measurable change in its spectral properties.

The Shaker-GFP fusion gene that we constructed reports changes in membrane potential by a change in its fluorescence emission. This fluorescence response is amplified in time over the electrical event, drastically increasing the optical signal power per event. Taken together, the properties of genetic encoding and temporal amplifications allow the sensor to be delivered to selected cells in which action potentials may be detected with standard imaging equipment.

2.2 Results

Fusion Constructs of the Shaker K⁺ Channel and GFP

Our goal was to construct a GFP-Shaker fusion protein in which Shaker retains normal conformational rearrangements, the fluorescence of GFP is correlated with these rearrangements, and the protein does not interfere with the physiology of the cells in which it is expressed. We were concerned that Shaker-GFP proteins could disrupt the physiology of the cells in which they were expressed by introducing an extra ionic current. Therefore, the point mutation *W434F* was engineered into the pore region of Shaker. This mutation prevents ion conduction but preserves the channel's gating rearrangements in response to voltage changes (Perozo, Santacruz-Toloza et al. 1994).

Since the core of the Shaker channel, including the N-terminal assembly domain and the transmembrane segments, is highly conserved (Stühmer, Ruppersberg et al. 1989; Drewe, Verma et al. 1992; Li, Jan et al. 1992; Shen, Chen et al. 1993) and therefore probably intolerant to large insertions, we fused GFP in-frame at a site just after the sixth transmembrane segment (S6; figure 2.1). The crystal structure of GFP indicates that its C-terminus is disordered from amino acids 230-238 (Ormö, Cubitt et al. 1996; Yang, Moss et al. 1996). Since several of these amino acids can be removed without disrupting GFP fluorescence (Dopf and Horiagon 1996), we deleted amino acids 233-238 (GFP Δ C) with the idea that the structured, fluorescent core of GFP could be tied directly to the moveable parts of the channel (Figure 2.1).

Xenopus laevis oocytes injected with cRNA transcribed from Shaker-W434F/ GFP Δ C@S6 (henceforth called FlaSh, for fluorescent Shaker) showed green membrane fluorescence (Figure 2.1C),

indicating that GFP was targeted appropriately. As expected, the *W434F* mutation abolished ionic current through the sensor. Voltage steps from a holding potential of -80 mV evoked only “on” and “off” gating currents (Figure 2.2A). Integrating the gating current gives the total charge (Q) moved during the voltage step. The time course of this gating charge movement reveals a fast component in response to small voltage steps and a slow component in response to larger voltage steps. The slow off currents following large depolarizations had the properties described earlier for the wild-type channel, in which inactivation by the N-terminus retards the return of the gating charge (Bezanilla, Perozo et al. 1991). We concluded that FlaSh retains the normal Shaker-like gating rearrangements in response to changes in membrane potential.

Voltage-clamp fluorimetry revealed that, remarkably, FlaSh changes its emission intensity in response to voltage steps. Depolarizing steps that moved the slow component of the gating charge and immobilized the off gating charge evoked a decrease in fluorescence from FlaSh (Figure 2.2A). A maximum fluorescence decrease of $5.1\% \pm 0.7\%$ ($n=7$) was observed in response to steps that moved all of the gating charge. Small depolarizing voltage steps, which evoked only the gating charge component that was minor and fast, produced no fluorescence change. The relation of the steady-state fluorescence change to voltage was sigmoidal and correlated closely with the steady-state gating charge-to-voltage relation (Figure 2.2B). This correlation indicates that, in FlaSh, the fluorescence emission of GFP is coupled to the voltage-dependent rearrangements of the Shaker channel.

The FlaSh protein was very stable, as judged by gating current and fluorescent measurements. Expression did not decline over a period of 2 weeks in *Xenopus* oocytes. Moreover, no bleaching was visible after >5 minutes of measurement with nearly continuous broadband (425-475nm) excitation. In addition, FlaSh continued to respond to voltage when we increased the temperature from 22°C to 37°C . The rates of both the onset and recovery of the fluorescence change were increased by 2.0 ± 0.3 ($n=3$) –fold at the higher temperature.

Kinetics of FlaSh

Although the fluorescence of FlaSh follows the voltage dependence of Shaker activation, the kinetics of the on and off fluorescence changes (F_{on} and F_{off}) were slower than the movement of the gating

charge (Q_{on} and Q_{off} ; compare F and Q in Figure 2.2A). At steps to 0 mV, Q_{on} was ~30-fold faster ($P < 0.0001$) than F_{on} ($\tau_{[Q-\text{on}]} = 2.8 \pm 0.4$ ms, $\tau_{[F-\text{on}]} = 85 \pm 10$ ms; $n = 5$). The slower kinetics of the fluorescence change indicate that rearrangement in the voltage sensor of Shaker may trigger but does not directly cause the change in GFP fluorescence.

The fluorescence response of FlaSh cannot be a direct consequence of N-type inactivation because F_{on} and F_{off} were slower than the onset and recovery of N-type inactivation. As shown earlier (Bezanilla, Perozo et al. 1991), the onset of gating charge immobilization, and thus N-type inactivation, closely followed Q_{on} (Figure 2.3, I_g), which was more than an order of magnitude faster than F_{on} . Moreover, the immobilized Q_{off} at -80 mV, following large depolarizations, returned approximately twice as fast ($P < 0.001$) as F_{off} ($\tau_{[Q-\text{off}]} = 72 \pm 7$ ms, $\tau_{[F-\text{off}]} = 160 \pm 12$ ms; $n = 7$).

The delay in the fluorescence change may arise from a time-dependent event in GFP, or a slow rearrangement in Shaker. The fluorescence change lacks intrinsic voltage sensitivity, whatever its mechanism, since the time constants of both F_{on} and F_{off} saturate at voltages outside of the voltage range of activation (Figure 2.2C).

Stereotypical Fluorescence Output from FlaSh Expands Brief Membrane Transients

To determine whether FlaSh could respond to short-lasting electrical activity, we explored its fluorescence kinetics in response to brief voltage pulses. These voltage transients moved a fraction of the total gating charge, and steps of 3 ms and longer evoked long, stereotypical fluorescent responses (Figure 2.3). While the magnitude of the fluorescence change was related to the duration of the step, its kinetics of onset and recovery were constant. The entire collection of fluorescent responses was well fit by a double-exponential with time constants of 23 ms for F_{on} and 105 ms for F_{off} . These kinetics are, respectively, 4-fold and 1.5-fold faster than those of the fluorescence changes evoked by longer steps.

This stereotyped fluorescence response was clearly visible in single-sweep recordings (Figure 2.4). Subsequent events that occurred during the time course of the fluorescence change summated with the original response. The unitary responses were visible in the summated response when the trains of

electrical events were at frequencies of 20 Hz or less. Trains of 100 Hz produced fused response in which the individual events could not be distinguished by eye (but see Discussion).

FlaSh Behaves Like a Linear Filter during Spike Trains

For a short train of identical brief pulses, the integral of the fluorescence response was constant at frequencies of 20 Hz and lower (Figure 2.4H) but declined at higher frequencies. The decline occurred as the peak response approached the maximal fluorescence change, i.e., as the sensor population became saturated. In the low frequency range, a linear filter model with the kinetics of the unitary response based on the stereotypical shape of the FlaSh fluorescence change (Figure 2.3) accounted well for the shape of the fluorescence response to a pulse train (Figure 2.4f and 2.4G). Given the acceleration of FlaSh kinetics when temperature is increased from 22°C to 37°C, the maximal firing rate over which FlaSh will be linear may be twice the frequency cutoff of the cooler temperature.

FlaSh Behaves Like a Linear Filter during Spike Trains

For a short train of identical brief pulses, the integral of the fluorescence response was constant at frequencies of 20 Hz and lower (Figure 2.4H) but declined at higher frequencies. The decline occurred as the peak response approached the maximal fluorescence change, i.e., as the sensor population became saturated. In the low frequency range, a linear filter model with the kinetics of the unitary response based

2.3 Discussion

We have constructed a gene fusion of GFP and the Shaker K⁺ channel that changes fluorescence emission in response to changes in membrane potential. The FlaSh protein encoded by this gene makes a stable, bleach-resistant optical voltage sensor with voltage dependence, kinetic properties, and fractional fluorescence change that should make it useful for the study of fast and slow electrical signaling.

Physiological Impact on Target Cell

To prevent FlaSh from altering the physiology of cells in which it is expressed, we made a point mutation in the Shaker pore that prevents ion conduction. While this works well in oocytes, expression of FlaSh in other cells may introduce the difficulty of FlaSh subunits coassembling with compatible subunits of the same subfamily of channels (Christie, North et al. 1990; Isacoff, Jan et al. 1990; McCormack, Lin et al. 1990; Ruppertsberg, Schröter et al. 1990; Covarrubias, Wei et al. 1991) and altering the properties of native channels. This may be avoided by linking cDNAs in such a way that the subunits of the channel are covalently attached (Isacoff, Jan et al. 1990). While we have not tested FlaSh in mammalian cells, we expect it to work just as well, given the high levels of expression of both Shaker and GFP in a variety of mammalian cell lines. (For a description of our attempts to make tandem constructs, see Chapter 3.)

Rearrangements Underlying the Change in FlaSh Fluorescence

What causes the fluorescent response of FlaSh? The fluorescence output clearly depends on Shaker activation. However, neither activation nor N-type inactivation can be directly responsible for inducing the fluorescence change, because these processes occur with a much faster time course. Since channel opening normally precedes N-type inactivation (Zagotta, Hoshi et al. 1990), this gating step is also likely to be too fast to directly cause the fluorescence change.

This leaves slower gating rearrangements of the channel, such as those underlying C-type inactivation (Timpe, Jan et al. 1988; Hoshi, Zagotta et al. 1990). Indeed, the kinetics of the fluorescence change were consistent with that of C-type inactivation in their voltage dependence (Figure 2.2C). As with the onset of C-type inactivation (Hoshi, Zagotta et al. 1991), the rate of F_{on} did not change with steps to voltages more positive than -30 mV; and as with the recovery of C-type inactivation in physiological solution (Levy and Deutsch 1996), the rate of F_{off} varied little at voltages more negative than -90 mV. Interestingly, depolarizations as short of 3 ms evoked fluorescent changes with $\tau_{[F-on]}$ of 23 ms, indicating that the conformational change responsible for the fluorescence change was triggered by the voltage transient but continued to build up long after the transient was over. This could be explained by the fact that N-type inactivation prevents the channel from deactivating (by immobilizing the gating charge) and

thus extends the time over which C-type inactivation can take place to beyond the end of the depolarization (Baukrowitz and Yellen 1995).

Taken together, these results indicate that the characteristic fluorescence response of FlaSh is initiated by the gating charge movement that accompanies channel activation or by N-type inactivation, but that the mechanism, and therefore the time course, is independent of these processes. Instead, the fluorescence change of FlaSh could be due to C-type inactivation or to another rearrangement in Shaker. Alternatively, the fluorescence change could be due to a slow rearrangement within GFP or to a slow change in the interaction between two or more GFPs in the four subunit channel complex. With regard to this last possibility, oligomerization of GFP does appear to affect its spectral properties (Ward, Prentice et al. 1982).

Whatever the direct cause of its fluorescence change, four functional states seem to account for the general behavior of FlaSh. Membrane depolarization rapidly pumps the sensor population from a bright resting state (R^*) into a bright activated state (A^*), from which it slowly decays into a dim activated state (A). Repolarization deactivates the sensor from the dim activated state (A) into a dim resting state $\text{\textcircled{R}}$, from which it slowly returns to the resting bright state (R^*). The rate-limiting fluorescent response profile reflects this voltage-independent redistribution of the population of sensors following the voltage-dependent gating events.

How Will FlaSh Report on Neural Activity

FlaSh is not a typical fluorescent voltage probe. Traditional “fast” voltage-sensitive dyes have been designed to respond quickly and linearly to membrane potential (Cohen and Leshner 1986; Gross and Loew 1989; Tsien 1989). By contrast, FlaSh provides a different solution to the underlying problem of detecting fast voltage transients: FlaSh gives long, stereotypical fluorescence pulses in response to brief voltage spikes.

The dynamic range of Flash is approximately -50 to -30 mV, for depolarizations that are long enough to allow the Shaker channel population to equilibrate. Short depolarizations that do not allow the gating to reach steady state produce smaller responses at any given voltage. Thus, depolarizations just a

few milliseconds in duration that are as large as an action potential (~ 40 mV) activate only a fraction of the sensor population and evoke submaximal responses. Whether the depolarizations are long or short, FlaSh responds mainly to depolarizations that are above the typical threshold for action potential firing of -45 mV.

FlaSh Behavior during Spike Trains

Because brief voltage pulses produce long-lasting, sub-maximal responses, trains of such pulses – with interpulse intervals shorter than the 500 ms fluorescence recovery time – produced summated responses that were linearly related to the number and frequency of the pulses, making FlaSh into a spike averager (Figure 2.4). This provides an illustration of how FlaSh, located in excitable neuronal cell bodies and axons, is likely to report on repetitive action potential firing, since these are also invariant in amplitude and duration. The idea that FlaSh can detect action potentials with a 1 ms duration at 37°C is based on the fact that single pulses of 3 ms duration activate enough sensors to produce sizable changes in fluorescence at 22°C , and the kinetics of Shaker activation of a Q_{10} of >3 (Nobile, Olcese et al. 1997). In contrast to its characteristic response to action potential depolarizations, FlaSh responds to slower depolarizations – those that more closely resemble dendritic excitatory postsynaptic potentials – with a fluorescence that follows the amplitude and duration of the depolarization. These two forms of detection are very useful, because neural information is encoded in action potential timing and frequency, as well as in synaptic potential amplitude and duration.

Advantages of FlaSh for Detecting Individual Action Potentials

The dynamics of FlaSh provide significant advantages for detecting individual electrical events. Because individual spikes can be as short as 1 ms, it has been a difficult detection problem to resolve individual events with traditional fast voltage-sensitive dyes. The temporally expanded response of FlaSh gives a significant advantage in this respect, as the area under the response is ~ 30 -fold larger than the area under the input spike (converting units appropriately). This temporal amplification makes single spikes 30 times easier to detect than they would be with a fast dye with a comparable fractional fluorescence change.

Although the response from FlaSh extends over 100 ms, the resolution with which individual spikes can be resolved is significantly better than 100 ms. For example, by inspecting figure 2.4, it is possible to estimate when spikes occurred to within a few milliseconds. Visual inspection would become more difficult in cases where the background noise is relatively large, as will be the case when recording from small cells *in vivo*. Significantly better resolution can be achieved in these cases by using linear filter theory to design an “inverse” Flash, i.e., a linear filter that reconstructs an unknown spike train given the fluorescent output generated by FlaSh. An impulse train is an adequate approximation to a train of action potentials, because voltage spikes (<10 ms) are typically much shorter than the characteristic fluorescence response from FlaSh (>100 ms). A linear filter approximation is appropriate as long as the sensor population does not saturate in the active state. A linear matched filter (Haykin 1994) did succeed in recovering spike times to within at least 10 ms, even in the presence of significant amounts of noise (data not shown).

Flexible Operating Range and Targeting of Sensor

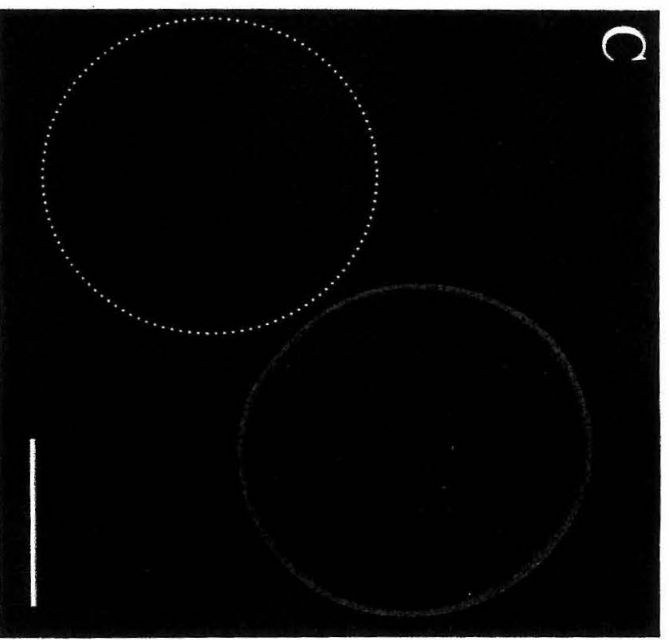
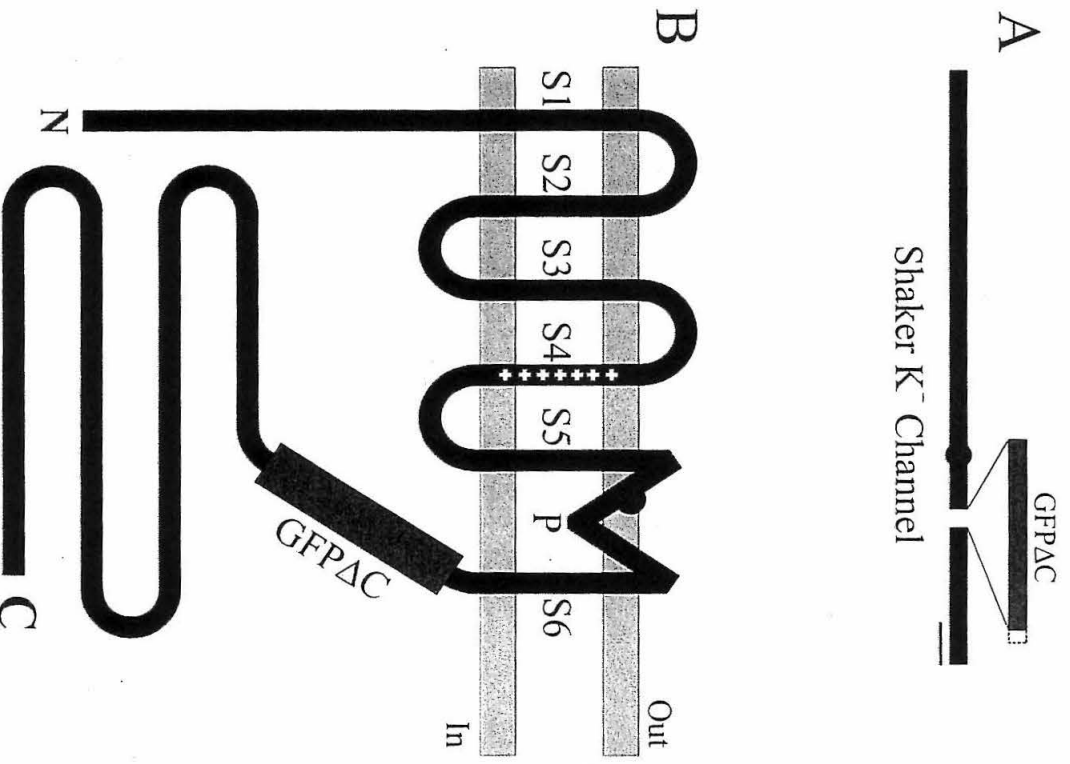
One advantage to using the Shaker channel is that many mutations have been described that produce unique alterations in its voltage dependence and kinetics. This provides flexibility in the design of optical voltage sensors with an operating range that best suits the signals of interest. For example, mutants with more negative operating range can be used to detect inhibitory and subthreshold excitatory synaptic activity, whereas mutants that operate at more positive potentials may be used to detect action potentials exclusively. (See chapter 3.)

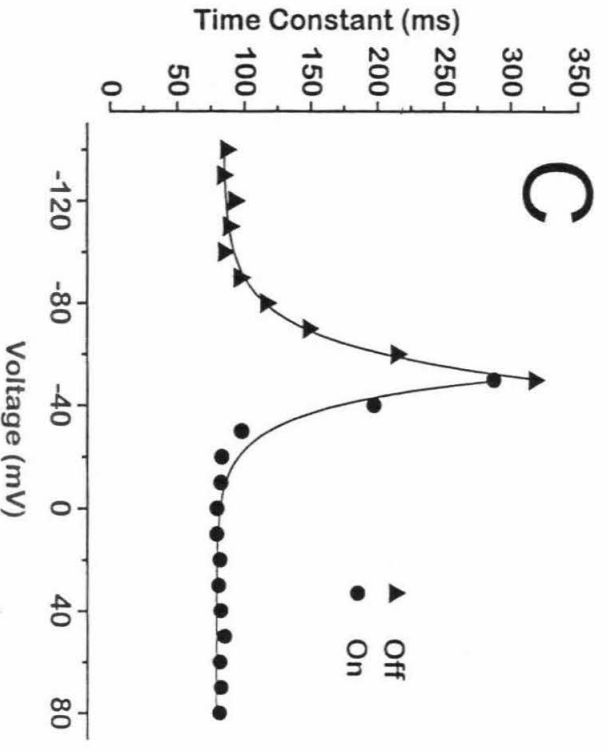
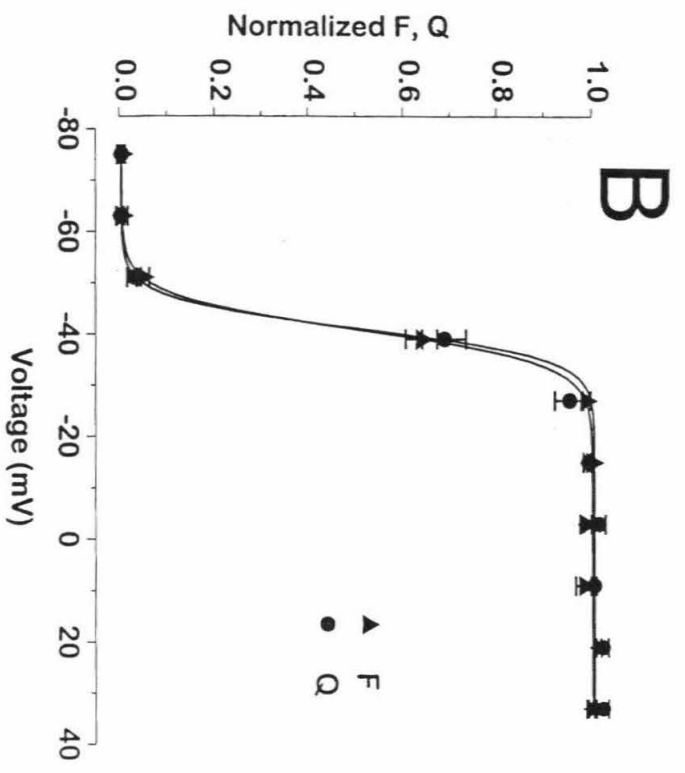
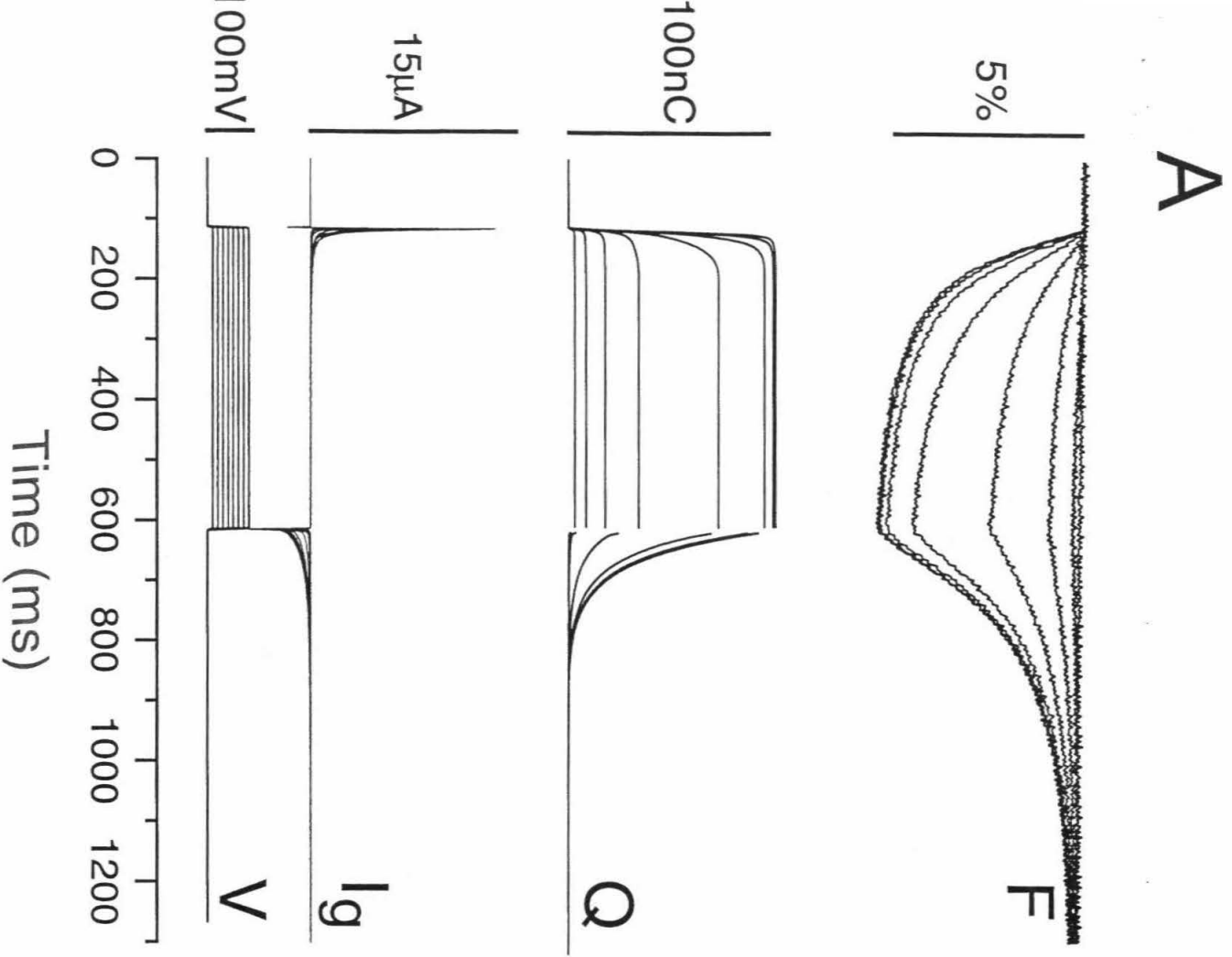
In the case of both passive dendrites or active axons, the magnitude of fluorescence change will be proportional to the excitatory activity. These two kinds of activity may be studied separately by selectively targeting FlaSh to dendrites, axons, or synapses. Heterologous proteins can be targeted to subcellular regions by genetically attaching peptide sequences that are localized by the transport machinery of the cell. This has been accomplished previously in several instances, including the synaptic localization of a membrane protein *in vivo* (Mostov, Apodaca et al. 1992; Callahan and Thomas 1994; Clark, Giniger et al. 1994; Zito, Fetter et al. 1997).

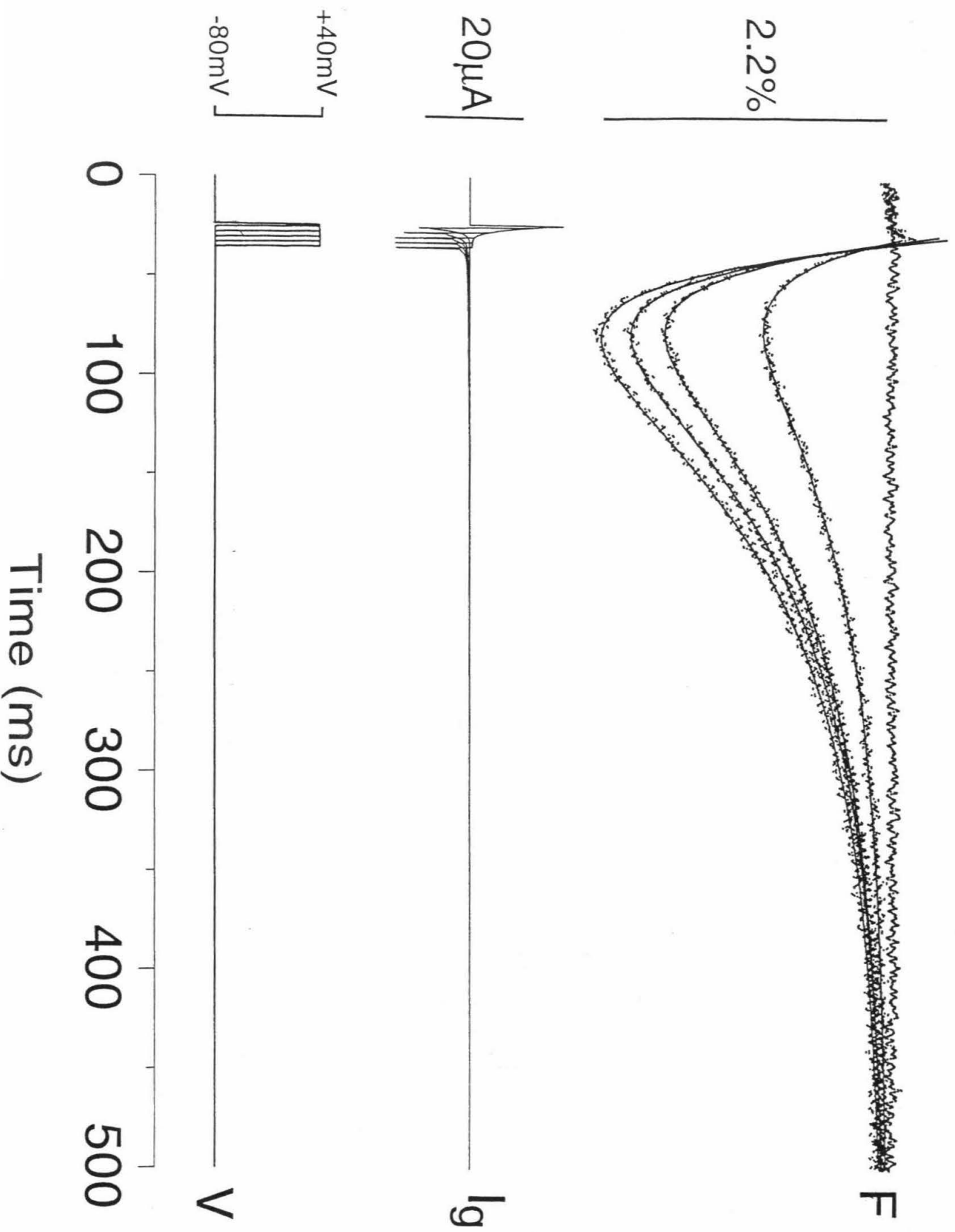
2.4 Conclusion

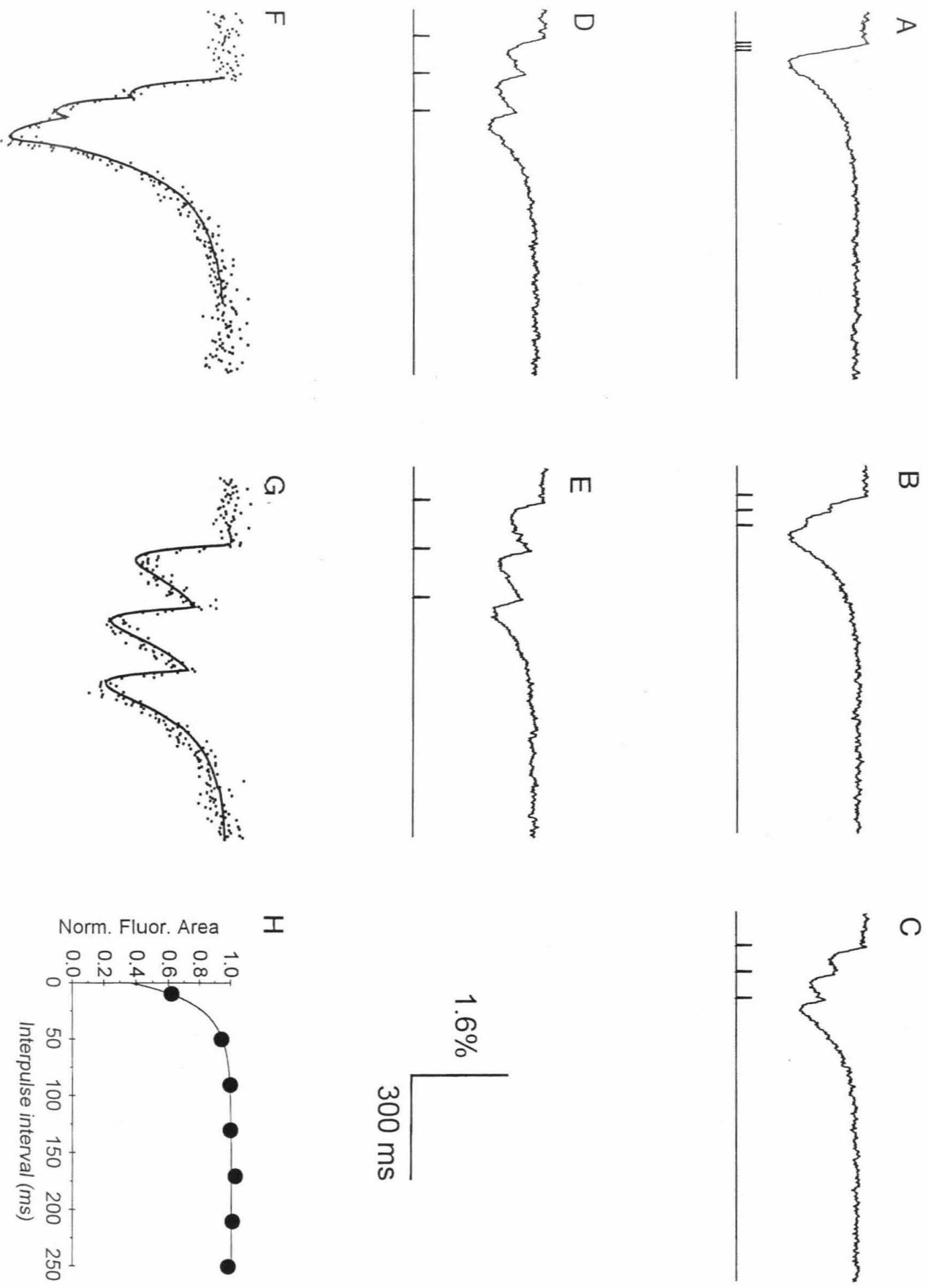
The success of the Shaker-GFP fusion protein as an optical voltage sensor suggests that the modular approach to the production of optical sensors may be expanded to the real-time detection of other signaling events. The constructs could include GFP Δ C as a reporter, a signal transduction protein as a detector, and, if desired, a subcellular targeting peptide. The most obvious variant of this would be to insert GFP Δ C just after S6 in cyclic nucleotide-gated channels or Ca²⁺-gated channels, so as to make a sensor for local, submembrane concentration of these second messengers. (See chapter five.) Such constructs may make possible the noninvasive detection of activity in a variety of proteins, including receptors, G proteins, enzymes, and motor proteins. The developmental timing and cellular specificity of expression can be controlled by placing the construct under the transcriptional control of a specific promoter. The combined ability to tune the sensor module via mutagenesis and to target the sensor to specific locations affords powerful advantages for the study of signal transduction events in intact tissues.

M.S. Siegel, Figure 1









Chapter 3

Modifications to FlaSh

In the previous chapter we have described a genetically encoded sensor (FlaSh) that measures membrane voltage and gives a green fluorescent output. The dynamic range of the FlaSh sensor is steep, from approximately -50 mV to -30 mV. For short membrane transients (e.g., sodium/potassium action potentials), its fluorescence output is a convolution of the membrane voltage with a fluorescence “impulse response.” We characterized some aspects of the sensor, most importantly, its impulse response and its dynamic range (-50 mV to -30 mV).

In the sections that follow, we will illustrate the response of the FlaSh sensor to physiologically realistic membrane transients. We will show an example of two cell types (salamander on-bipolar cells and cone cells) to which FlaSh is well suited. Then we will show that FlaSh is poorly tuned to respond to some other cell types (e.g., salamander amacrine cells). Finally, we will discuss mutations of the Shaker K⁺ channel that shift the dynamic range of Shaker. We tested these mutations in FlaSh and their effects will be presented.

3.1 Physiological effect of FlaSh on neurons

To prevent FlaSh from altering the physiology of cells in which it is expressed, we made the *W434F* point mutation in the Shaker pore to prevent ion conduction. This mutation blocks conduction by locking a gate in the pore into a closed conformation. Normally this gate closes slowly during sustained depolarization, producing slow inactivation. Other gating processes and rearrangements remain normal in the mutant channel, including activation in response to depolarization, opening of the activation gate, ball-and-chain (N-type) inactivation, and the rearrangement that consolidates slow inactivation and changes the fluorescence of GFP (Peroza et al. 1993; Bezanilla et al. 1994; Siegel and Isacoff 1997; Yang and Sigworth 1997; Loots and Isacoff 1998).

The use of the *W434F* mutation works to prevent ion conduction in non-excitabile cells, such as *Xenopus* oocytes, where FlaSh subunits are the only subunits from the Shaker K⁺ channel subfamily that are expressed, so that FlaSh channels form as non-conducting (permanently inactivated) homotetramers.

However, in excitable cells such as neurons and muscle, where native subunits from the Shaker subfamily (which carry the wildtype W at position 434) *are* expressed, FlaSh subunits may co-assemble with those native subunits to form heterotetramers. In such heterotetramers, the slow inactivation gate will shut more quickly than in wildtype (*W434*) homotetramers, meaning that the properties of the K⁺ conductances in the cell will be altered. Although the effect of altering one class of voltage-gated K⁺ channels through pharmacology is often subtle, heterotetrameric channels may nevertheless affect the functional properties of the cells — a side effect of sensor expression that would be better avoided.

Our approach to circumventing co-assembly between FlaSh and native channels in excitable cells is to link four FlaSh cDNAs in tandem in such a way that the four subunits of the channel are covalently attached (Isacoff, Jan et al. 1990). This approach has been used earlier to force subunits to assemble in a known stoichiometry (Hurst et al. 1992; Liman et al. 1992; Liu et al. 1996). The expectation is that linked FlaSh constructs should assemble into FlaSh homotetramers even in excitable cells because of the higher likelihood of intra-molecular assembly between linked FlaSh subunits than inter-molecular assembly with native channel subunits.

In an attempt to test this idea, we constructed four separate FlaSh constructs in which the FlaSh sensor is concatenated with itself or with the Shaker K⁺ channel alone, using two different linker sequences. These sensor designs are illustrated in Figure 3.1.

Unfortunately, we were unable to express these constructs in *Xenopus* oocytes, as measured by fluorescence or by electrical gating currents. This result is puzzling, because it is known that one can express Shaker-Shaker tandem constructs in oocytes, and that these tandem constructs behave normally. It has been found that expression levels of these constructs is lower by several-fold over the monomer. (Isacoff et al. 1990; Hurst et al. 1992; Liman et al. 1992; Liu et al. 1996). However, even with a ten-fold reduction in expression levels we would have expected to see the FlaSh-FlaSh tandem constructs, given the large and robust signal we get from the FlaSh monomer.

The difficulty we experienced in expressing FlaSh-FlaSh tandem dimers could have been due to the linker sequence. The two linker sequences we used to connect the C-termini of FlaSh to the N-termini of FlaSh were based on those sequences that had been successful for linking together Shaker-Shaker tandem dimers. It is unclear if the presence of GFP near the C-terminus of Shaker could hinder the

FlaSh tandem constructs

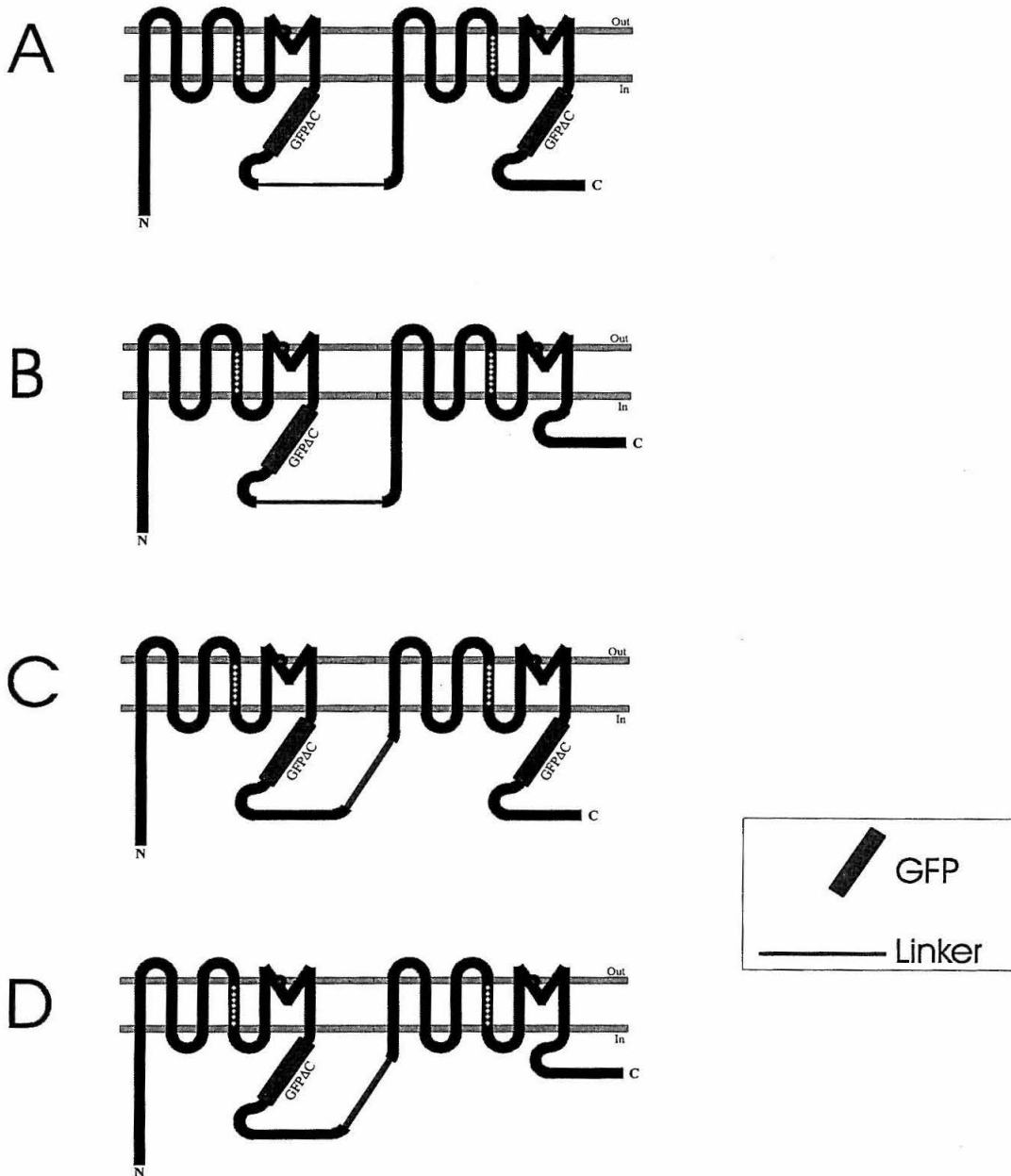


Figure 3.1. Tandem constructs. FlaSh-FlaSh and FlaSh-Shaker tandem constructs to encourage intramolecular subunit assembly. (A) FlaSh-FlaSh; (B) FlaSh-Shaker; (C) FlaSh-{FlaSh Δ (1-46)}; (D) FlaSh-{Shaker Δ (1-46)}.

assembly of the FlaSh-FlaSh tandem dimer constructs with these linkers, or inhibit their transportation to the membrane. It is possible that a longer linker would have been more successful.

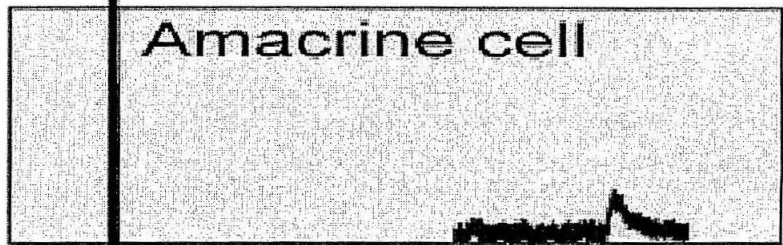
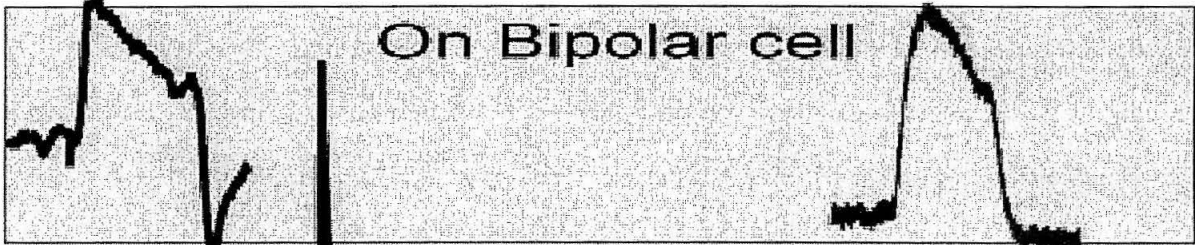
If one wanted to optimize the linker sequence to express FlaSh-FlaSh tandem dimers, it might make sense to do this in the conducting (*W434W*, rather than *W434F*) version of FlaSh, as the electrical signal of the conducting channel would be a sensitive assay for the amount of FlaSh-FlaSh dimer protein that was expressed and functional. Another approach would be to generate a random library of FlaSh-FlaSh tandem sensors proteins with different linker sequences, and then to screen this library for high expression (bright fluorescence) in mammalian cells. (See chapter 7.) Our experience is that synthesizing and testing different linker sequences is rather laborious; therefore, it is our feeling that the random approach could be more productive than optimizing the linker sequence rationally.

3.2 FlaSh response to retinal voltage transients

Given the narrow range of voltage over which Shaker channels gate, and over which FlaSh modulates its brightness (Figure 2.?), it is clear that some voltage signals will be reported more efficiently, while others may be missed altogether. Since mammalian neurons tend to rest at about -70 mV, small excitatory and inhibitory postsynaptic potentials will not fall within the dynamic range of FlaSh (-50 mV to -30 mV). However, suprathreshold excitatory postsynaptic potentials and action potentials should be reported.

We examined the response of FlaSh to physiologically realistic voltage traces. Voltage transients measured in response to light in a variety of salamander retinal cell types (Roska, Nemeth et al. 1998) were applied via a voltage clamp to oocytes expressing Flash. See Figure 3.2. Note that the fluorescent signal from FlaSh reflected the dynamics of cone cells and on-bipolar cell quite well. This is because the light-induced response of the cone cell and the on-bipolar cell is within the dynamic range of FlaSh (-50 mV to -30 mV), and because the FlaSh impulse response is significantly faster than the time-scale of the voltage transient (1 sec).

As an aside, note that sustained illumination on the salamander retina induced a “sag” current in on-bipolar cells. The signal from Flash captures this “sag” on-bipolar response.



Voltage



Fluorescence



FlaSh dynamic range is not optimal for some cell types

We also explored the response of FlaSh to membrane transients recorded in other cell types. Flash did not capture the response of salamander wide-field amacrine cells or horizontal cells, because the main response of these cell types occurs from -70 mV to -50 mV, outside of its dynamic range. Note in Figure 3.2 that FlaSh reflects only the peak of the voltage transient in amacrine and horizontal cells, at those times when the voltage trajectory passes through the dynamic range of FlaSh. Clearly FlaSh misses important features of the dynamic response in these cell types.

3.3 Shifting the dynamic range of FlaSh through mutagenesis

One advantage of using the Shaker channel is that many mutations have been described which produce unique alterations in its voltage dependence and kinetics. This provides flexibility in tuning FlaSh to an operating range that best suits the signals of interest. For example, the dynamic range of Shaker channel gating is from approximately -30 mV to -50 mV. It is known that the mutation L366A [Lopez et al. (1991)] in the S4 region of the Shaker channel shifts channel gating toward hyperpolarized potentials -50 mV to -70 mV.

We have made versions of FlaSh with a more negative operating range based on this mutation. We engineered the point mutation L366A into FlaSh using site directed mutagenesis (Sambrook, Fritsch et al. 1989). We measured the dynamic range of these sensors using voltage-clamp fluorimetry, as we did for FlaSh. This result is shown in figure 3.3 Note that the dynamic range of L366A-FlaSh is shifted by 20 mV and that the fluorescence change and gating currents are shifted in parallel. This is exactly what would be expected from effects of the L366A point mutation on Shaker gating.

L366A FlaSh provide a good optical sensor for measuring the voltage waves from wide-field amacrine cells and horizontal cells as shown in Figure 3.4.

Point Mutation Shifts Dynamic Range of FlaSh

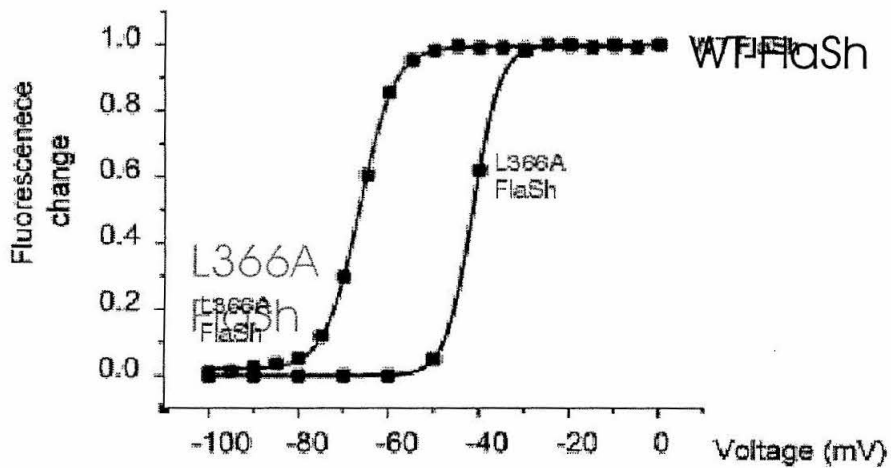
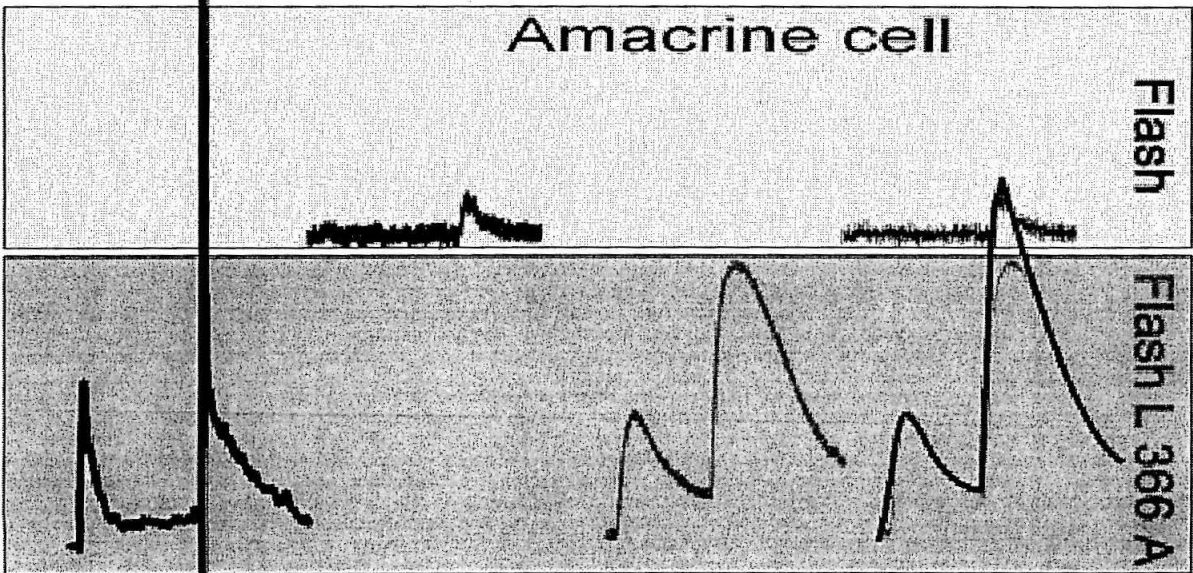
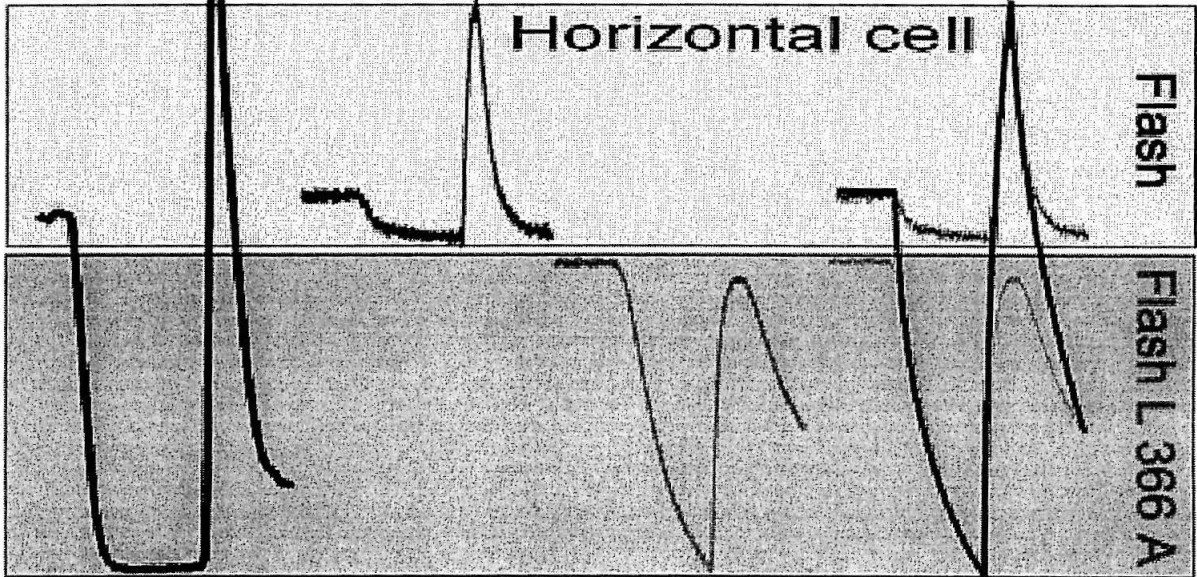


Figure 3.3. Point mutation shifts the dynamic range of FlaSh. Fluorescence change measured in response to voltage steps applied to oocytes expressing $\{\Delta 6-46\}$ -FlaSh or L366A- $\{\Delta 6-46\}$ -FlaSh. Voltage steps between -100 mV and 0 mV from -80 mV. Dynamic range of FlaSh is approximately -50 mV to -30 mV. Dynamic range of L366A-FlaSh is approximately -70 mV to -50 mV.

Flash

Flash
L 366 A

Flash
Flash
L 366 A



3.4 Fast FlaSh: deleting the “inactivation ball” of Shaker

What causes the fluorescent response of FlaSh? The fluorescence output clearly depends on Shaker activation. However, neither activation nor N-type inactivation can be directly responsible for inducing the fluorescence change, because these processes occur with a much faster time course. Since channel opening normally precedes N-type inactivation (Zagotta, Hoshi et al. 1990), this gating step is also likely to be too fast to directly cause the fluorescence change.

It is curious that short voltage transients in FlaSh produce long fluorescence pulses.

As discussed in chapter two, depolarizations as short as 3 ms evoked fluorescent changes with $\tau_{[F_{on}]}$ of 23 ms in FlaSh, indicating that the conformational change responsible for the fluorescence change was triggered by the voltage transient but continued to build up long after the transient was over. We suggested that this could be explained by the fact that N-type inactivation prevents the channel from deactivating (by immobilizing the gating charge) and thus extends the time over which C-type inactivation can take place to beyond the end of the depolarization (Baukrowitz and Yellen 1995).

It is known that the N-terminal ball of Shaker can be removed, and that this deleted channel { $\Delta 6-46$ }-Shaker exhibits neither N-type inactivation nor gating charge immobilization (Zagotta, Hoshi et al. 1990). However, the deleted channel does exhibit C-type inactivation (Timpe, Jan et al. 1988; Hoshi, Zagotta et al. 1990).

In order to explore the possibility that gating charge immobilization is responsible for the long fluorescence pulse in FlaSh, we deleted the N-terminal “ball” from Flash. For the ball-deleted sensor, { $\Delta 6-46$ }-FlaSh, one would predict that the fluorescence change should return coincident with the re-polarization of the membrane.

As shown in Figure 3.5, this is exactly what we found. We applied short pulses of increasing duration to { $\Delta 6-46$ }-FlaSh. The downward fluorescence change begins when the membrane is depolarized. By contrast to wtFlaSh, the fluorescence returns when the membrane is repolarized. (By comparison, examine Figures in chapter 2 for wildtype FlaSh.) One could notice that the envelope of { $\Delta 6-46$ }-FlaSh in

Figure 3.5 corresponds to the shape of the fluorescence change from FlaSh in response to long voltage steps.

This result suggests that gating-charge immobilization is the mechanism by which short voltage transients in FlaSh produce long fluorescence pulses. Additionally, the $\{\Delta 6-46\}$ -FlaSh could be useful for measuring from cell-types where it is important to capture the dynamics of the “off response.” In those cases, gating-charge immobilization might obscure the fluorescence response from wt-FlaSh. However, for cells where one is interested in measuring fast action potentials, the drawn out fluorescence pulse of wtFlaSh provides the advantage of temporal amplification. Temporal amplification in FlaSh is discussed at length in Chapter 2.

3.5 Slow FlaSh: modulating “C-type inactivation” of Shaker

The results discussed above indicate that the characteristic fluorescence response of FlaSh is initiated by the gating charge movement that accompanies channel activation or by N-type inactivation, but that the mechanism, and therefore the time course, is independent of these processes. Instead, the fluorescence change of FlaSh could be due to C-type inactivation or to another rearrangement in Shaker.

If the fluorescence change in FlaSh is initiated by a process related to C-type inactivation, then mutations that alter the rate of C-type inactivation should alter the rate of fluorescence onset in FlaSh. We tested this by introducing the mutation C462A into the $\{\Delta 6-46\}$ -FlaSh channel. C462A is known to consolidate channel inactivation by stabilizing the P-type inactivated state. (Olcese, Latorre et al. 1997; Loots and Isacoff 1998).

Because C462A channels undergo C-type inactivation more slowly, we would predict that this mutation should slow down the fluorescence change in FlaSh. The response of C462A- $\{\Delta 6-46\}$ -FlaSh in response to a voltage step from -80 mV to $+20$ mV is shown in Figure 3.6 As predicted, C462A- $\{\Delta 6-46\}$ -FlaSh is slower than wt-FlaSh by several fold. This result suggests that C-type inactivation could be involved in the fluorescence change we see in FlaSh. However, the mutation probably is not useful for a sensor *in vivo*, because in almost every case one would prefer to increase the speed of the response from FlaSh.

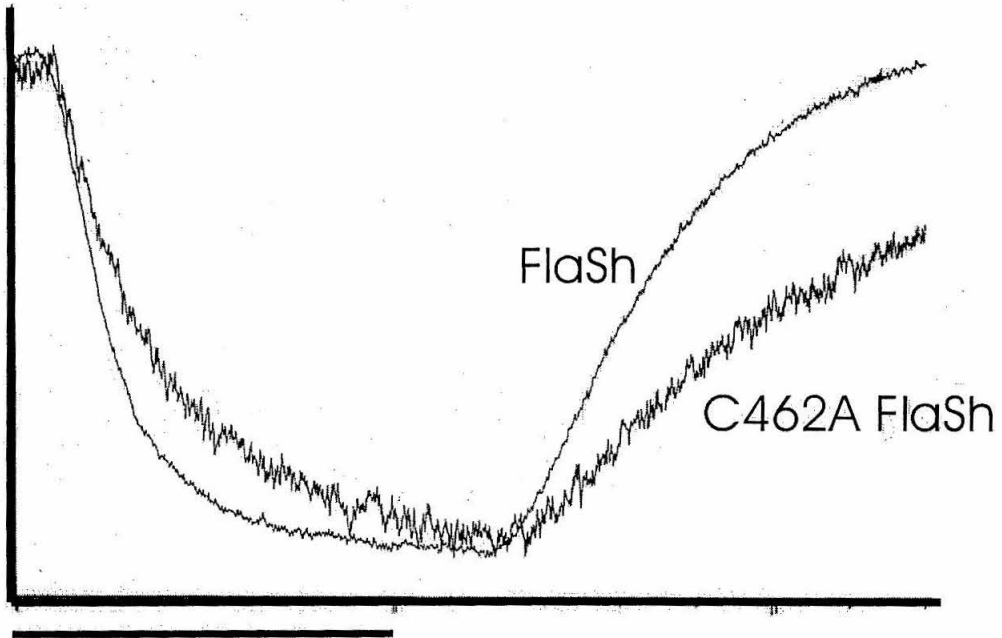


Figure 3.6 Mutations that modulate Shaker inactivation also modulate FlaSh fluorescence. C462A-FlaSh is significantly slower than FlaSh for voltage steps from -80 mV to 0 mV. C462A is known to slow entry into “c-type” inactivated state of Shaker. Note the slow recovery of fluorescence in C462A-FlaSh. Fluorescence traces are normalized to emphasize kinetics of response. Scale bar, 500 msec.

3.6 Methods for making chimeric sensors

Making N- and C- terminal fusion proteins

A large literature exists on methods for concatenating two genes together to make a single fusion protein (Sambrook, Fritsch et al. 1989). These methods vary in detail. Typically, as shown in figure 3.7, one uses restriction enzymes and DNA ligase to insert the first gene into a commercial vector that is optimized for N- or C-terminal fusion constructs (Step I). Then, using this backbone, one can insert the second gene into the N- or C- terminal polylinker (Step II). One needs to be careful that the second protein lands “in-frame” with the first protein, in order that the chimeric product retains one translational frame (Step III). Often, the commercial vector has been optimized for this purpose. Finally, one removes extraneous stop and start codons residing in the middle of the fusion protein. These can be removed when the gene fragment is amplified (prior to its insertion) using PCR. Alternatively, one can remove these extraneous sites in the final product using site-directed mutagenesis.

These methods do not solve the general problem of inserting one gene into another.

We developed a simple method for inserting GFP into a protein of interest. The method works well for inserting GFP into a variety of predetermined locations. To use this method, one should have some intuition about structural properties of the target. For example, we inserted GFP into a variety of locations in Shaker, guided by our knowledge about regions of Shaker that undergo conformational rearrangements in response to membrane voltage.

Making chimeric genes with Splicing by Overlap Extension (SOE)

In general, one would like a method for creating chimeric proteins that is not limited to N- and C-terminal fusion constructs. There is some literature on using the Splicing by Overlap Extension (SOE) reaction to concatenate two genes. This method is not limited to terminal fusion proteins. For example, see (Horton, Hunt et al. 1989; Warrens, Jones et al. 1997). An outline of this method is shown in Figure 3.8. Typically, one amplifies the desired product in segments, using overlapping (“sticky”) tails (Step I). Then one extends the partial intermediate products in 1:1:1 molar ratio (Step II, Step III) and temperature cycles to generate the full length chimeric gene (Step IV).

We attempted to use this method to insert GFP into several locations in the Shaker potassium channel. None of the chimeric genes was successfully expressed in oocytes, as measured by physiology or fluorescence.

There is at least one frustrating problem with using the SOE method: the chimeric gene can be thrown out of frame at arbitrary locations during annealing/extension of the intermediate products (Step III). In practice, we found that automated DNA sequencing is useful for determining errors or mutations at a **particular** location. However, automated DNA sequencing is too noisy to determine whether there has been any single insertion or deletion **anywhere** in any SOE junction. As a result, one never has confidence in a negative result, since one always wonders if it is caused by an out-of-frame error in the product.

Making chimeric genes with polymerase chain reaction and mutagenesis

Ultimately, we returned to a simple but reliable method for inserting GFP into the Shaker potassium channel at arbitrary locations. (See Figure 3.9.) In this method, we choose a restriction site (e.g., SpeI) that does not exist in GFP, in the vector, or in the polylinker. If the site did exist at one or a few locations, the site could have been voided using site-directed mutagenesis. Usually, this can be done in a way that does not alter coding sequence of the gene.

1. Mutagenesis: we choose a location in Shaker where we want to put GFP. We insert the consensus sequence for SpeI (ACTAGT) into Shaker at that location. This is done using standard site-directed mutagenesis procedure. Typically, we use ten to fifteen bases on either side of the insertion site to ensure stringent annealing during mutagenesis.

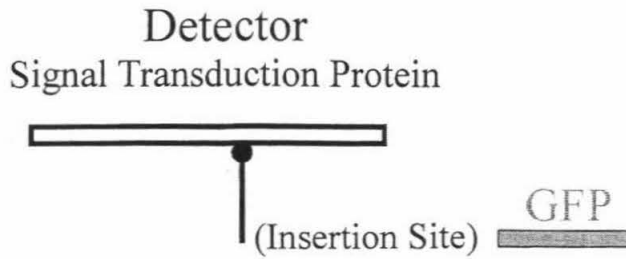
2. PCR: we use the polymerase chain reaction to amplify GFP with primers that contain the consensus sequence for SpeI. (CCTAGTAAAGGAGAAGAAGCTTTC and GGACTAGTGCCATGTGTAATCCCAGCAGCTGT). Note that amplifying with these primers has the effect of removing the start codon and the stop codon from GFP. In this example, we also remove fifteen basepairs from the C-terminus of GFP (to form GFP Δ C). We also include CC and GG sequences at the 5' end of the primers in order to form a "GC" clamp. Note that the clamp falls off from the product during the next step.

3a. Digestion: we use SpeI restriction enzyme to digest the PCR product (GFP Δ C) and the target (Shaker). At this point it is helpful to remove phosphate groups from the target using calf intestinal phosphatase. Phosphatase treatment prevents the target from re-ligating without GFP in the next step.

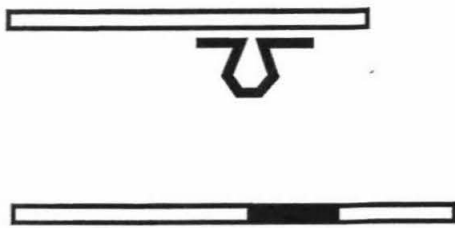
3b. Ligation: we mix GFP and Shaker in a molar ratio that encourages ligation of the insert into the target, and add ligase. (Typically this ratio is about 5:1::insert:vector).

4. Screening: we transform the population of DNA into bacteria, plate out single colonies, and screen the colonies. We isolate those constructs in which a single GFP has been inserted into Shaker at the desired location.

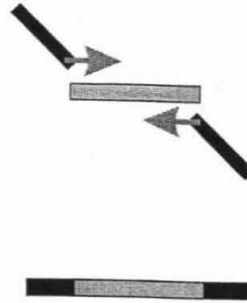
Chimeric Genes: Mutagenesis coupled PCR



1. Mutagenesis



2. PCR amplification



3. Digestion / Ligation



4. Screen for Correct Product



Figure 3.9 Chimeric proteins by mutagenesis coupled to PCR. See text for explanation.

There are at least two caveats with the method of mutagenesis coupled to PCR: 1. GFP can ligate in either the forward or reverse directions, 2. GFP can concatamerize. Typically, we examine several clones to screen for those constructs in which a single GFP is inserted in the correct (forward) orientation. We screen these by a secondary PCR reaction in which one primer is internal to GFP and one primer is internal to Shaker. This diagnostic PCR can be performed directly on the bacterial stab. (No need to isolate DNA!) Only clones with a single GFP inserted in the correct orientation will produce a single PCR product of the expected size. Other constructs produce no band, or produce a band of a size that is incorrect.

For example, we followed this procedure to insert GFP into a SpeI site in the Shaker K⁺ channel. Diagnostic PCR was performed on ten individual colonies, directly from agarose gel plates. Figure 3.10 shows the result of this PCR reaction. One PCR primer was internal to GFP and one PCR primer was in Shaker. Note that it is simple to screen for colonies in which GFP has landed in the correct orientation. (In this case 4/10 colonies are positive.) It is helpful to do a positive control reaction with a Shaker-GFP construct and two negative control reactions, without primers and without the bacterial template, respectively. PCR gives a reproducible product that is easily seen on the gel. The clear signal is typical of the diagnostic reaction.

Alternatively, we have screened clones by restriction enzyme digestion with NcoI, which cuts at the beginning of Shaker and at the beginning of GFP. DNA fragments can be distinguished on an agarose gel, corresponding to the case of forward and reverse GFP insertions. Finally, one can determine that only a single GFP has been inserted into Shaker by linearizing the clone with the restriction enzyme HpaI, which cuts once in GFP, and does not cut Shaker or the vector.

Note that the multiple chimeric proteins can be created and tested in parallel, in separate tubes. For example, one can make different insertion sites in Shaker or one can insert differently colored GFP variants. In practice, we find that one can create up to about ten constructs in parallel without significantly increasing the time required for the process.



Figure 3.10 Example of mutagenesis coupled PCR. We created ten FlaSh constructs. These were tested using a diagnostic PCR reaction with one primer internal to Shaker and one primer internal to GFP. (See text.) Clones #2,#3,#7,#10 are positive for GFP in the correct orientation. Positive control and negative controls were successful as well.

Finally, note that the method of mutagenesis coupled PCR is less useful when nothing is known about the target protein. In that case, it is more interesting to approach the problem using combinatorial methods to screen large libraries of chimeric proteins (see Chapter 6).

Conclusion

Using the method of mutagenesis coupled PCR, we have inserted GFP Δ C, eGFP Δ C, eYFP Δ C, eCFP Δ C, uvGFP Δ C (Tsien 1998), and ratiometricGFP Δ C (Miesenböck, De Angelis et al. 1998) into over eight locations in Shaker and into a variety of other channel proteins. (See figure 3.11). Many of these constructs did not glow in oocytes and did not give rise to functional gating currents. Several of the constructs were fluorescent and gave rise to gating currents, but there was no correlation between the electrical signal and fluorescent signal from the chimeric protein. Only a few constructs demonstrated coordinate changes in fluorescence and electrical signals in response to membrane voltage. Some of these results are discussed in the sections that follow.

3.7 Chimeric proteins between GFP and Shaker K⁺ channel

In this section we will describe the qualitative behavior of several chimeric membrane proteins. We created these proteins by inserting GFP Δ C into a variety of locations in Shaker. We find that GFP Δ C can be inserted at the N-terminal, at the C-terminal, and also at a variety of internal sites. In our experience, these chimeric proteins are usually fluorescent and electrically normal relative to the ShH4W4343F channel. The tolerance of many proteins to GFP insertion is probably due to the structure of GFP, in which the N- and C- termini emerge in close proximity to one another on the same side of the barrel structure (Ormö, Cubitt et al. 1996).

In general, GFP insertion points near the N- and C- termini of the Shaker protein seemed to be better tolerated. We were not successful at inserting GFP Δ C into the loops between membrane-spanning helices of Shaker. We did not attempt to insert GFP near the pore region of Shaker, as the pore is highly conserved among members of the Shaker protein family and single amino acid mutations in the pore are known to disrupt the function of Shaker.

All constructs are in the *W434F* background, which blocks ionic conduction through the Shaker channel. All constructs were tested using cRNA injection followed by two electrode voltage clamp and fluorescence measurement in *Xenopus* oocytes (Siegel and Isacoff 1997).

1. GFP Δ C inserted into N-terminus of Shaker

Amino Acid: 2 in Shaker.

We inserted GFP Δ C into the N-terminus of Shaker. This protein exhibited normal gating currents and a bright green fluorescence was visible at the oocyte membrane. We observed no correlation between the fluorescence output and the membrane voltage or gating state of the channel. We did not see any correlation between the fluorescence of GFP Δ C and fast-inactivation of Shaker. Shaker gating currents were normal, including charge immobilization following sustained depolarizations, which is related to the N-terminal “ball” region of Shaker (Bezanilla, Perozo et al. 1991). We had hoped that the fluorescence of this protein might be sensitive to fast-inactivation of Shaker because of the proximity of GFP Δ C to the fast-inactivation “ball.”

Inserting GFPAC into ShakerH4

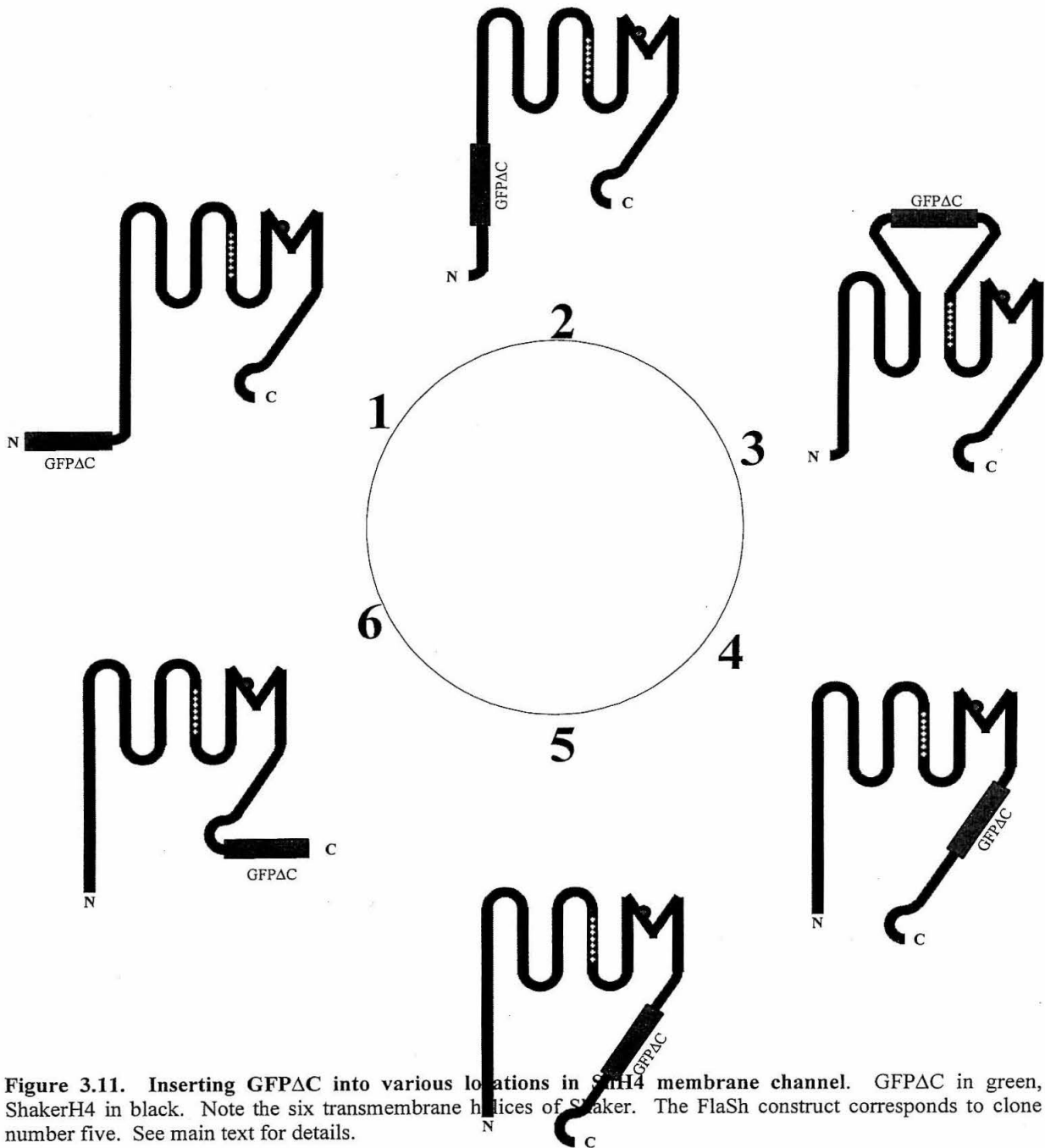


Figure 3.11. Inserting GFPAC into various locations in ShakerH4 membrane channel. GFPAC in green, ShakerH4 in black. Note the six transmembrane helices of Shaker. The FlaSh construct corresponds to clone number five. See main text for details.

2. GFP inserted into N-terminus between “ball” and T1 domain of Shaker

Amino Acid: 131 in Shaker.

This was inspired by the partial success of N-terminal fusion of GFP Δ C. We inserted GFP Δ C into the region of Shaker between the N-terminal “ball” and the N-terminal “T1 assembly domain” of Shaker (Bezanilla, Perozo et al. 1991; Li, Jan et al. 1992). This protein behaved identically to the N-terminal GFP Δ C-Shaker fusion. As with the N-terminal fusion, we observed no correlation between the fluorescence output and the membrane voltage or gating state of the channel. We did not see any correlation between the fluorescence of GFP Δ C and fast-inactivation of Shaker. Shaker gating currents were normal, including charge immobilization following sustained depolarizations, which is related to the N-terminal “ball” region of Shaker (Bezanilla, Perozo et al. 1991). It is interesting that the presence of GFP near T1 evidently did not disrupt the tetrameric assembly of Shaker.

3. GFP between S3 and S4 transmembrane helices of Shaker

Amino Acid: 349 in Shaker.

Using the method of splicing by overlap extension, we inserted GFP Δ C into three locations between transmembrane helices three and four of Shaker. We were unable to measure gating currents or fluorescence from any of these constructs. Based on the membrane topology of Shaker, these proteins should have located GFP Δ C on the external face of the membrane, which could have been a problem for GFP Δ C expression. We had hoped the fluorescence of this protein might be sensitive to the gating movement of the S4 helix, because it is known that this helix moves through the cell membrane during channel gating [Baker et al, 1996].

We did not attempt to insert GFP between the S4 and S5 transmembrane helices. The S4/S5 region is highly conserved across the Shaker family. The loop between S4/S5 in Shaker has been shown to act as an intracellular receptor for the Shaker N-terminal “ball” during fast inactivation (Isacoff, Jan et al. 1991). Also, based on homology between Shaker-like proteins, the S4/S5 loop appears intolerant to small insertions. (See figure 3.12.)

4. GFP inserted near membrane after S6 region of Shaker

Amino Acid: 493 in Shaker.

We inserted GFP Δ C into one location between the sixth transmembrane helix of Shaker and the native SpeI site. These constructs were inspired by our success with FlaSh (see below). We had hoped that we might see a larger ΔF or faster kinetics by inserting GFP near the insertion point in FlaSh. We saw a reversible downward change in fluorescence in response to membrane voltage depolarizations. However, the size of this signal and its kinetics were essentially identical to the signal from FlaSh. The fluorescence output followed the voltage dependence of channel gating, as it does in FlaSh.

5. GFP inserted at SpeI site after S6 region of Shaker: FlaSh

Amino Acid: 503 in Shaker.

We inserted GFP Δ C into the native SpeI site in Shaker. This protein (FlaSh) exhibited normal gating currents, and a bright green fluorescence was visible at the oocyte membrane. This protein is characterized at length in other chapters. Briefly, we saw a reversible change in fluorescence in response to membrane voltage changes. We believe that the fluorescence response is triggered by a slow rearrangement in Shaker that requires gating charge immobilization. The fluorescence output perfectly follows the voltage dependence of channel gating. As shown in other chapters, the output is modified in parallel with channel gating by mutations that alter the channel's dynamic range or kinetics.

<i>Location</i>	<i>Site in ShH4 / Method</i>	<i>Electrical?</i>	<i>Fluorescence?</i>	ΔF
N-terminus of ShH4	/MCPCR	Yes	Yes	None
Between N-terminal "ball" and "T1" of ShH4	/MCPCR	Yes	Yes	None
S3/S4 loop of ShH4	/SOE	No	No	None
Between S6 & SpeI in ShH4	/MCPCR	Yes	Yes	Yes (5%)
FlaSh (native SpeI site after S6 in ShH4)	/MCPCR	Yes	Yes	Yes (5%)
C-terminus of ShH4	/MCPCR	Yes	Yes	None

Table 3.13 Effect of inserting GFP Δ C into various locations in ShH4 membrane channel. All successful insertion points were intracellular. Fluorescence was measured with epifluorescence using an HQGFP filter (Chroma Technologies). Electrical (gating) currents were measured using two-electrode voltage clamp. ΔF refers to a change in fluorescence from the baseline fluorescence level. MCPCR = mutagenesis coupled PCR; SOE = splicing by overlap extension. Insertion site is measured from the ShH4 start codon, in units of units of one amino acid. See main text for details.

6. GFP Δ C inserted into C-terminus of Shaker

Amino Acid: 656 in Shaker.

We inserted GFP Δ C into the C-terminus of Shaker. The protein exhibited normal gating currents and a bright green fluorescence was visible at the oocyte membrane. We observed no correlation between the fluorescence of GFP Δ C and the membrane voltage or gating states of the channel. It is interesting that this protein was able to be translocated to the plasma membrane. The Shaker channel contains a PDZ-interaction domain at its C-terminus that is known to target Shaker preferentially to post-synaptic specializations (Tejedor et al., 1997; Zito et al 1997, 1999). In principle, GFP Δ C could have disrupted the C-terminal targeting sequence of Shaker.

Conclusion

We have found that it can be helpful to examine sequences from a wide variety of homologous proteins (e.g., comparing Shaker, Shab, and Shaw K^+ channels). Often homology can yield insight into those regions in the protein sequence which are highly conserved through evolution, and which therefore might be intolerant to GFP insertions. For example, we never were able to make functional proteins in which GFP was fused into regions near the fourth transmembrane segment (S4) in Shaker. We had hoped that this region would be interesting because of the high homology between S4 transmembrane segments in a variety of channel proteins, and because the Shaker S4 segment is known to undergo conformational rearrangements in response to transmembrane voltage. Unfortunately, the Shaker channel was intolerant to GFP insertions in three regions between the S3 and the S4 helices. These fusion proteins were neither fluorescent nor did the channel function, implying that the GFP insertion interfered with protein folding, assembly or stability.

In general, we were surprised at the tolerance of ShakerH4 to GFP Δ C insertion at a variety of locations. Most of these proteins were fluorescent and electrically normal. However, in only a few cases was the fluorescence of GFP Δ C dependent on the electrical activity of Shaker.

One approach to improving the size of the fluorescence change (ΔF) might be insert GFP Δ C at a range of locations near its insertion point in FlaSh. Another approach would be to use fluorescence resonance energy transfer between two different color variants of GFP (e.g., eCFP and eYFP) located on different Shaker subunits or at different locations on the same Shaker subunit. (We pursued the second strategy in some detail. See chapter four.)

Chapter 4. FlaSh with altered spectra

4.1 A review of fluorescent proteins

The two best-characterized fluorescent proteins are from marine invertebrates: a Pacific Northwest jellyfish, *Aequorea victoria*, and a sea pansy from the Georgia coastline, *Renilla reniformis*. These proteins absorb blue chemiluminescence from a distinct primary photoprotein and emit green fluorescence. More recently, (Matz, Fradkov et al. 1999) have cloned yellow and red-orange emitting fluorescent proteins from the fluorescent but non-bioluminescent corals of the Indian and Pacific oceans.

The first written report of bioluminescence was from Pliny the Elder in the first century AD, who wrote about a glowing marine creature in the Bay of Naples (Johnson and Shimomura 1978; Cubitt, Heim et al. 1995). This work was suspended due to unfavorable funding conditions and the eruption of Vesuvius in AD79. More recently, biochemical studies of various GFPs began in the 1960s in the laboratories of Blinks, Cormier, Hastings, Johnson and Shimomura, Prendergast and Ward. Their work culminated in the cloning of a cDNA (gfp10) encoded *Aequorea* GFP (Prasher, Eckenrode et al. 1992). (Chalfie, Tu et al. 1994) galvanized widespread interest in GFP by showing that the recombinant gene remains fluorescent when expressed in a variety of cell types. Subsequently, many groups have shown that GFP can be used as a marker of individual cells and can be tagged to a diverse range of proteins to follow their movements within a cell. (Reviewed in (Cubitt, Heim et al. 1995).)

4.2 Structure of GFP

Soon after the cloning and heterologous expression of the *Aequorea* cDNA, its structure was solved by x-ray crystallography (Ormö, Cubitt et al. 1996; Yang, Moss et al. 1996). *Aequorea* GFP is a 238 amino acid protein of 27,000 Mr. As shown in Figure 4.1, the structure reveals a novel “ β -can” fold, in which an eleven-stranded β -sheet has been wrapped around a central alpha-helix. *Aequorea* GFP owes its visible absorbance and fluorescence to a hexapeptide “antenna” that is buried in the center of the β -can structure. The antenna is formed from a post-translational cyclization of Ser65, Tyr66 and Gly67 along the central alpha-helix. This cyclization process is temperature dependent and the subsequent maturation of the chromophore requires molecular oxygen. [Reviewed in Cubitt, 1995 #9].

Once it has cyclized and matured, the GFP protein is highly stable and highly protease resistant, remaining fluorescent even at pH 11, 65°C, 1% SDS (Ward, Prentice et al. 1982). Denatured GFP protein or isolated GFP peptides absorb light but are practically nonfluorescent. Under some conditions after denaturation it is possible to renature GFP and recover its fluorescence (Ward, Prentice et al. 1982).

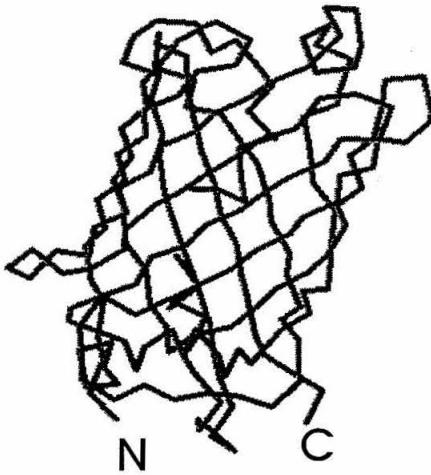
Dimerization: GFP from the sea pansy, *Renilla reniformis*, exists as a tight dimer. (Cutler and Ward 1993) As shown by (Ward, Prentice et al. 1982), and suggested by its crystal structure (Yang, Moss et al. 1996), *Aequorea* GFP also has a tendency to dimerize. This can be detected as a partial suppression of the 475 nm excitation peak. It is tempting to conjecture that a monomer/dimer transition could be involved in the fluorescence change we see in the FlaSh sensor: four GFP barrels are presumably packed together in close proximity around the tetrameric Shaker channel. Also, fluorescence energy transfer experiments suggest that the mutual orientation or distance between GFPs is altered during the fluorescence transition in FlaSh. (See chapter 5)

Circular Permutation: (Baird, Zacharias et al. 1999) have shown that GFP can be circularly-permuted and that some of these permuted variants retain their fluorescence. Furthermore, Baird et al. demonstrate locations in GFP that are tolerant to large peptide and even small protein insertions, where structural rearrangements in the inserted protein give rise to fluorescence changes in GFP. This is remarkable, as (Dopf and Horiagon 1996) had shown previously that only one residue from the amino terminus and ten residues from the carboxyl terminus can be deleted from wtGFP. Circular permutation is a promising avenue for developing environmentally sensitive variants of GFP. It might be interesting to explore whether these circularly permuted versions could be placed into FlaSh to increase the size of the induced fluorescence change.

Other Fluorescent Proteins: (Matz, Fradkov et al. 1999) describe the cloning and analysis of yellow and red-orange emitting fluorescent proteins. Like *Aequorea* GFP, these proteins are naturally fluorescent in a variety of cell types. This work is especially interesting because though these proteins contain only 26-30% sequence identity to *Aequorea* GFP, several features of the GFP structure appear to have been conserved, including the 11-stranded “ β -can” fold, many segments within the first β -turn and the caps of the can, and Arg96 and Glu222, the residues that interact most strongly with the chromophore. (Tsien 1999)

Molecular Structure of GFP

Side



Top

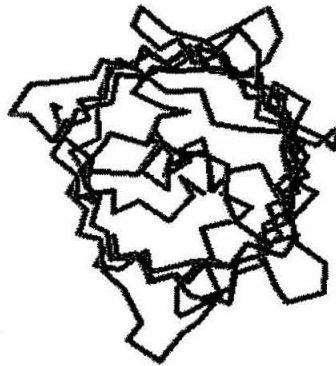


Figure 4.1. Molecular Structure of *Aequorea victoria* GFP GFP(S65→T) rendered by RasMol from Protein Data Bank Structure 1EMA. GFP is an eleven-stranded beta barrel folded around a central helix. The barrel forms a nearly perfect cylinder 42 Å long and 24 Å in diameter. The central helix collapses to make the chromophore, which is locked in the center of the barrel.

Engineering GFP for brightness and stability

Brightness: As described by (Heim, Cubitt et al. 1995), a single mutation from Ser65→Thr markedly alters the excitation spectra of GFP, nearly abolishing the 395 nm absorption peak and shifting the longer (475 nm) wavelength excitation peak to 490 nm. This mutation confers several other advantages, including: 1. about sixfold greater brightness than wild-type when each is excited at its longest-wavelength peak; 2. fourfold faster oxidation; 3. no photoisomerization and greatly decreased photobleaching (Heim and Tsien 1996).

Thermostability: While the mature GFP is highly stable in vitro, the autocatalytic reaction that produces the chromophore appears to be temperature sensitive. This is consistent with the idea that the *Aequorea victoria* exists in a cold ocean environment; therefore, one would presume that GFP has not evolved to retain function at higher temperatures. The temperature-sensitivity of GFP maturation is a significant problem for expressing *Aequorea* GFP in mammalian cells and in other cells that require higher incubation temperatures. For example, it was shown by (Simering, Golbik et al. 1996) that GFP can be as much as 20-fold “less fluorescent” when expressed in bacteria and yeast grown at 37°C rather than at 25°C.

Toward this end, Simering et al. and others discovered mutations such as Val163→Ala and Phe64→Leu that greatly suppress this thermosensitivity of GFP maturation. In addition, it has been found to improve the expression of GFP in many systems to “humanize” the GFP codon usage to align more closely with the relative tRNA concentrations that are present in mammalian cells (Zolotukhin, Potter et al. 1996). Both of these improvements have been widely useful for visualizing GFP in vivo.

4.3 Altering the spectrum of GFP

Variants of GFP with different colors would be useful for simultaneous comparisons of multiple protein fates, developmental lineages, or different gene expression levels. Many groups have described mutations that alter the excitation or emission spectrum of *Aequorea* GFP. Some of these mutations are compiled and reviewed in (Heim and Tsien 1996). In addition, the crystal structures of five variants have been solved by x-ray diffraction and molecular displacement (Palm, Zdanov et al. 1997).

The sequence of four independent wtGFP genomic clones are compared in figure 4.2. Some interesting mutations are taken from (Heim and Tsien 1996) and entered in the space below the sequence, along with a description of their spectral effects. Note the hexapeptide FSYGVQ that forms the chromophore, and the commonly used S65→T mutation in this sequence. Renilla refers to GFP isolated from a sea pansy from the Georgia coastline, *Renilla reniformis*, whose chromophore sequence has been determined by protein sequencing (though the full sequence of *Renilla* GFP is not yet published). The excitation spectrum of *Renilla* GFP closely resembles that of *Aequorea* GFP S65→T.

AevGFPa (M62653)	MSKGEELFTGVVPILVELDGDVNG H KFSV	29
AevGFP (L29345)	MSKGEELFTGVVPILVELDGDVNG Q KFSV	
GFP, Unpub. (X83959)	MSKGEELFTGVVP V LVELDGDVNG Q KFSV	
GFP, Unpub. (X83960)	MSKGEELFTGVVPILVELDGDVNG Q KFSV	
AevGFPa (M62653)	SGEGEGDATYGKLT L TKFICTTGKLPVPWP	58
AevGFP (L29345)	SGEGEGDATYGKLT L TKFICTTGKLPVPWP	
GFP, Unpub. (X83959)	SGEGEGDATYGKLT L N FICTTGKLPVPWP	
GFP, Unpub. (X83960)	R GEGEGDATYGKLT L TKFICTTGKLPVPWP	
AevGFPa (M62653)	TLVTTFSYGV Q CFSRYPDHMK R HDFFKSA	87
AevGFP (L29345)	TLVTTFSYGV Q CFSRYPDHMK Q HDFFKSA	
GFP, Unpub. (X83959)	TLVTTFSYGV Q CFSRYPDHMK Q HDFFKSA	
GFP, Unpub. (X83960)	TLVTTFSYGV Q CFSRYPDHMK Q HDF L KSA	
"6xGFP:"	T	
"Renilla:" DR	
AevGFPa (M62653)	MPEGYV Q ERTIF F KDDGNYKTRAEVKFEG	116
AevGFP (L29345)	MPEGYV Q ERTIF F KDDGNYKTRAEVKFEG	
GFP, Unpub. (X83959)	MPEGYV Q ERTIF F KDDGNYKTRAEVKFEG	
GFP, Unpub. (X83960)	MPEGYV Q ERTIF F KDDGNYKTRAEVKFEG	
AevGFPa (M62653)	DTLVNRIELK G IDFKEDGNILGHK L EYNY	145
AevGFP (L29345)	DTLVNRIELK G IDFKEDGNILGHK L EYNY	
GFP, Unpub. (X83959)	DTLVNRIELK G IDFKEDGNILGHK L EYNY	
GFP, Unpub. (X83960)	DTLVNRIELK G IDFKEDGNILGHK L EYNY	
AevGFPa (M62653)	NSHNVYIMADK Q KNGIKVNF KI RHNI E DG	174
AevGFP (L29345)	NSHNVYIMADK Q KNGIKVNF KI RHNI K DG	
GFP, Unpub. (X83959)	NSHNVYIM G DKPKNGIKVNF KI RHNI K DG	
GFP, Unpub. (X83960)	NSHNVYIM G DKPKNGIKVNF KI RHNI K DG	
AevGFPa (M62653)	SV Q LADHY Q QNTPIGDGPVLLP D NHYLST	203
AevGFP (L29345)	SV Q LADHY Q QNTPIGDGPVLLP D NHYLST	
GFP, Unpub. (X83959)	SV Q LADHY Q QNTPIGDGPVLLP D NHYLST	
GFP, Unpub. (X83960)	SV Q LADHY Q QNTPIGDGPVLLP D NHYLST	
"S202F, T203I (390nm excit):"	. . . FI	
AevGFPa (M62653)	Q S ALSKDPNEKRD H MVLL E FVTAAGITH G	232
AevGFP (L29345)	Q S ALSKDPNEKRD H MVLL E FVTAAGITH G	
GFP, Unpub. (X83959)	Q S ALSKDPNEKRD H MVLL E FVTA A R I TH G	
GFP, Unpub. (X83960)	Q S AL S Q DP H G KRD H MVLL E FV T S AGITH G	
"E222G (470nm excit):"	. . . G . .	
AevGFPa (M62653)	MDELYK	238
AevGFP (L29345)	MDELYK	
GFP, Unpub. (X83959)	MDELYK	
GFP, Unpub. (X83960)	MDELYK	

Figure 4.2. Sequences of *Aequorea victoria* GFP. Sequence comparison of four GFP clones from GenBank. 64FSYGVQ hexapeptide forms the chromophore. Synthetic mutations along with their spectral effects are listed below the sequences. Vertical lines indicate mRNA splicing sites in *Aequorea* genomic DNA. (Note the unappreciated fact that GFP contains an RNA splice site in its chromophore. Interesting!)

As an aside, we observe that, like many genomic sequences, *Aequorea victoria* contains mRNA exons and introns that are spliced together to form a complete GFP. The mRNA splicing process in the jellyfish has not been studied to our knowledge. **It is interesting that one splice site occurs in the hexapeptide that forms the chromophore.** This seems an unusual coincidence to us; one wonders if its presence suggests a possible mechanisms by which the jellyfish regulates its own fluorescence.

4.4 Useful GFP variants for FRET: eYFP, eCFP, eGFP

Fluorescence resonance energy transfer (Stryer 1978) is another application for differently colored GFP variants. Fluorescence resonance energy transfer (FRET) is a process whereby one fluorescent molecule can be excited indirectly *via* a second fluorescent molecule. Efficient FRET requires that the emission spectra of one molecule overlaps the excitation spectra of the other. The effect depends strongly on the distance between two fluorescent molecules and on their relative orientation. As a consequence, resonance energy transfer can be used to amplify small steric changes within a protein into large changes in fluorescence.

(Heim and Tsien 1996) and (Mitra, Silva et al. 1996) have used FRET between differently colored fluorescent proteins to monitor protease activity *in vitro*. Both groups engineered protease consensus sequences into a synthetic linker connecting two GFP variants. Proteolytic cleavage at the consensus sequence disrupted energy transfer between the molecules, so that the proteolysis reaction can be monitored directly.

In a beautiful paper, (Miyawaki, Llopis et al. 1997) describe sensors based on FRET that can be used to measure calcium concentration *in vivo*. Miyawaki et al. connected two GFP variants with a linker composed of calmodulin and the calmodulin-binding peptide M13. Binding of Ca^{2+} makes calmodulin wrap around the M13 domain, increasing the FRET efficiency between the two GFPs. Miyawaki et al. call this sensor “cameleon” because it changes color and retracts and extends a long tongue (M13) into and out of the mouth of the calmodulin (CaM).

The excitation and emission spectrum of several commercially available GFP variants are shown in figure 4.3. Note the overlapping emission spectra from eCFP (F64L / S65T / Y66W / N146I / M153T / V163A / N212K) and excitation spectra of eYFP (S65G / S72A / T203Y). eCFP/eYFP make a good

donor/acceptor pair for FRET because of their excellent spectral overlap, their high quantum efficiency, and their low bleach rate. As shown in (Miyawaki, Llopis et al. 1997) for the cameleon sensor, it is possible to excite eCFP with short wavelength light (440 ± 10 nm) and monitor independently the emission from eCFP (480 ± 15 nm) and from eYFP (535 ± 12.5 nm). Recently, (Miyawaki, Griesbeck et al. 1999) improved on this pair by introducing the mutations V68L / Q69K to eYFP, which reduces the pH-sensitivity of eYFP.

For comparison, the excitation/emission spectra of eGFP (F64L/S65T), one widely used variant, is included in figure 4.3 as well. eBFP (F64L/Y66H/Y145F) has not been particular useful as a FRET donor because of its low quantum efficiency and its propensity to bleach.

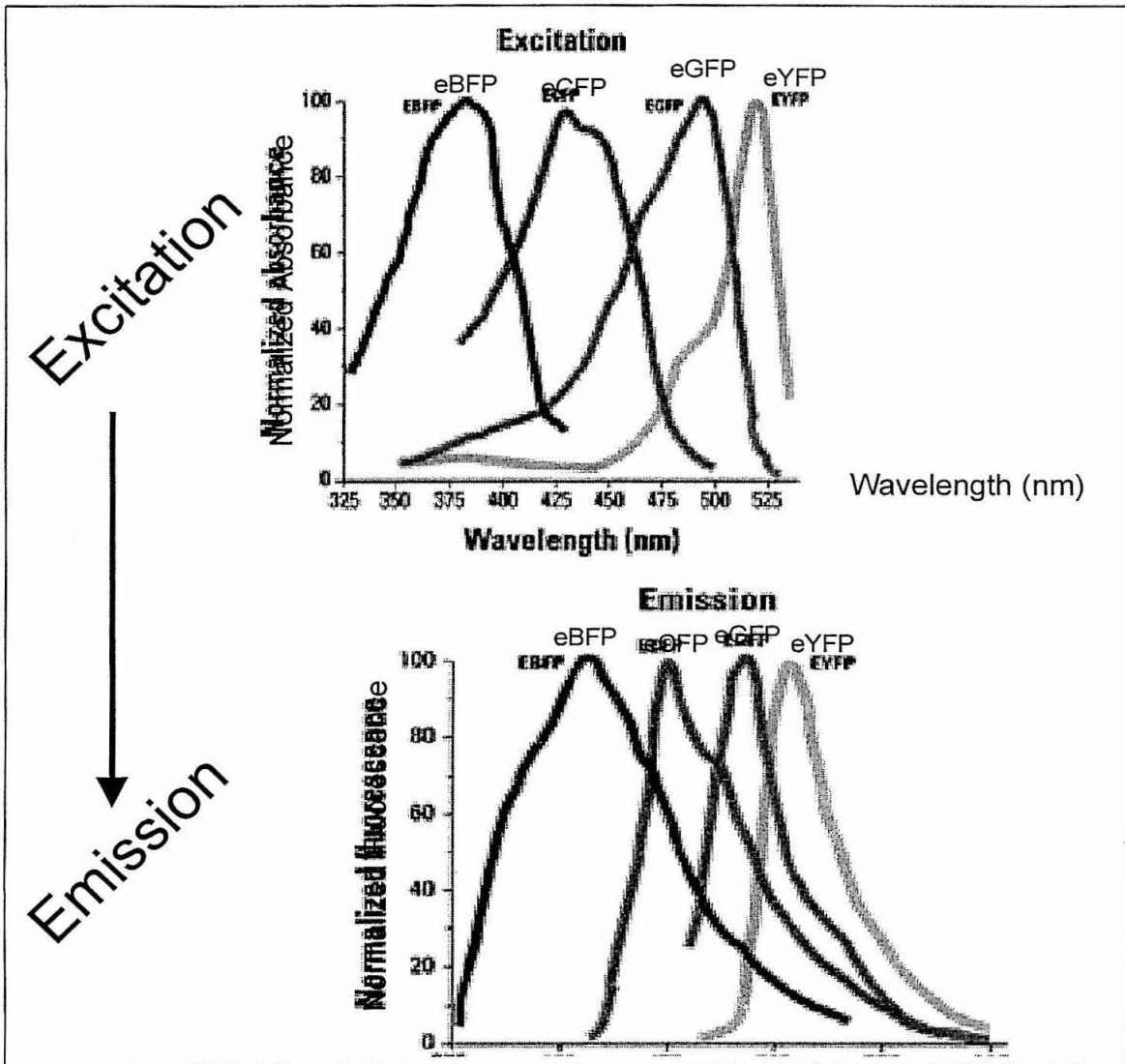


Figure 4.3. Excitation/Emission Spectra of GFP Variants. Data from Chroma, Inc.

4.5 FlaSh color variants

As discussed above, different GFP variants can display shifts in excitation spectra, emission spectra, and sensitivity to pH (Miesenböck, De Angelis et al. 1998; Miyawaki, Griesbeck et al. 1999). For this reason, we were curious to measure the qualitative behavior of chimeric proteins in which these GFP variants have been fused into the Shaker channel.

In this section we summarize the behavior of wtGFP Δ C, eGFP Δ C, eYFP Δ C, and eCFP Δ C variants inserted into the endogenous SpeI site of the Shaker channel using mutagenesis coupled PCR. The endogenous SpeI site is the location in Shaker (near the sixth membrane helix) that we used to create the FlaSh sensor. These results are summarized in Table 4?. Measurements were made under two different filter sets: HQ-GFP (excitation filter, 425-475 nm; dichroic, 480 nm long-pass; emission filter, 485-535 nm); and HQFITC (excitation filter, ?? nm; dichroic, ?? nm long-pass; emission filter, ?? nm)

wtGFP–FlaSh

As shown in previous chapters, FlaSh is wtGFP Δ C inserted into the endogenous SpeI site in Shaker. The FlaSh protein exhibits a voltage-dependent decrease in fluorescence of approximately 5% when measured with an HQ-GFP filter cube. When measured with HQ-FITC cube, FlaSh gives XXX.

eGFP–FlaSh

As discussed earlier, a single mutation from Ser65 \rightarrow Thr markedly alters the excitation spectra of GFP, nearly abolishing the 395 nm absorption peak and shifting the longer (475 nm) wavelength excitation peak to 490 nm. In addition, this GFP variant is about six fold brighter than wild-type GFP when each is excited at its longest-wavelength peak. We had hoped that eGFP Δ C inserted into Shaker might yield a brighter FlaSh.

In fact, the overall fluorescence from eGFP Δ C-FlaSh is significantly brighter than wtGFP Δ C-FlaSh. However, its fluorescence change (ΔF) is diminished ten-fold under both HQ-GFP and HQ-FITC conditions as compared to wild-type FlaSh. A fluorescence representative trace from eGFP Δ C-FlaSh in response to voltage steps is shown in figure 4.4. The difference in behavior between wtGFP Δ C and

eGFP Δ C in the same location in Shaker might give insight into the mechanism responsible for the fluorescence change in FlaSh.

It is known from (Brejc, Sixma et al. 1997) that the two absorption maxima in wtGFP are caused by a change in the ionization state of the chromophore. The equilibrium between these states appears to be governed by a hydrogen bond network that permits proton transfer between the chromophore and neighboring side chains, including Glu-222. The predominant neutral form of the fluorophore absorbs maximally at 395 nm. The ionized form of the fluorophore, absorbing at 475 nm, is present in a minor fraction of the native protein (Brejc, Sixma et al. 1997).

In the GFP S65 \rightarrow T (eGFP) structure, the fluorophore is permanently ionized, causing only a 489-nm excitation peak. It is unlikely that the deletion of the C-terminus (Δ 233-238) from GFP significantly alters the basic structure of GFP, as this region of the protein does not appear in any published crystal structure of GFP and it is evidently disordered.

One could speculate that, in FlaSh, the distribution between protonated and deprotonated states of the chromophore of GFP is altered during the fluorescence change. Presumably, eGFP-FlaSh is permanently locked in the ionized state and this could explain why we see a greatly reduced fluorescence change even though the overall protein is brighter. One way to resolve this question would be to conduct wavelength excitation and emission scan of FlaSh and eGFP-FlaSh during the fluorescence change.

If protonation/deprotonation is involved in the fluorescence change in FlaSh, we would expect that the relative size of the excitation peaks in FlaSh should be altered during the fluorescence change. Comparing the result from an HQ-FITC cube and an HQ-GFP cube is difficult, as the excitation bands overlap somewhat and do not clearly separate the two excitation peaks. Spectral scanning would be more precise.

eGFP-FlaSh Response is Very Small

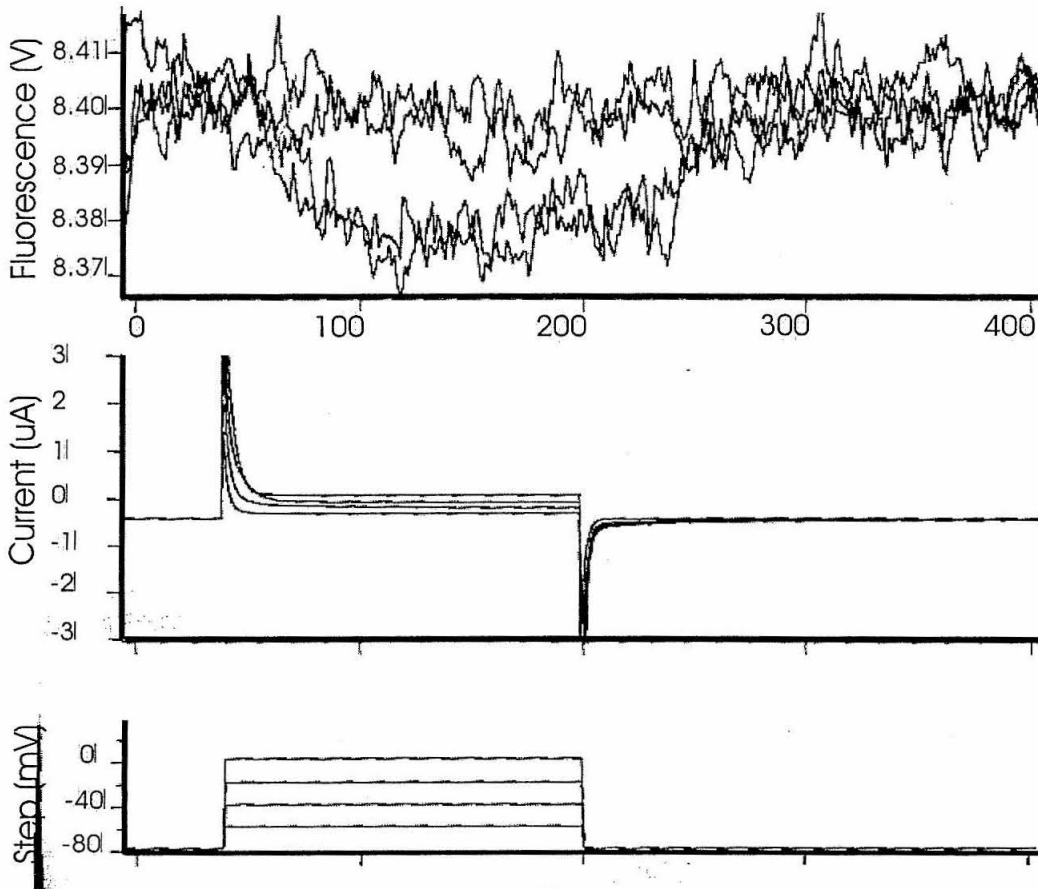


Figure 4.4 eGFP Δ C-FlaSh gives small response to membrane voltage steps. Simultaneous two-electrode voltage recording and photometry show current and fluorescence changes in response to voltage steps. Voltage steps (V) from -80 mV to $+0$ mV, in 20 mV increments. Holding potential was -80 mV. Note the maximal fluorescence change is only 0.3% , as compared to 5.0% for wtFlaSh. Fluorescence scale, 0.1% .

eCFP-FlaSh

We inserted eCFP Δ C into the endogenous Spe I site of Shaker. We know that the protein was expressed because we measured fluorescence at the oocyte membrane and measured large gating currents. However, we saw no fluorescence change in eCFP under HQ-GFP, HQ-FITC, or eCFP excitation. The last filter combination was optimized for the excitation and emission spectrum of eCFP.

eYFP-FlaSh

We inserted eYFP Δ C into the endogenous Spe I site of Shaker. We know that the protein was expressed because we measured fluorescence at the oocyte membrane and measured large gating currents. At first glance, we saw no fluorescence change in eYFP under HQ-GFP, HQ-FITC.

However, using longer depolarizations (5 sec), we measured a slow, upward fluorescence change (ΔF) in eYFP-FlaSh of approximately 4.9%. Representative traces from eYFP Δ C-Flash in response to voltage steps are shown in Figure 4.5. Note that the ΔF in eYFP-FlaSh is reversed in sign from the ΔF in FlaSh and that it is much slower. The size of this upward ΔF was sigmoidally related to the membrane depolarization and correlated with the amount of gating charge moved during the depolarization, similar to the ΔF in FlaSh.

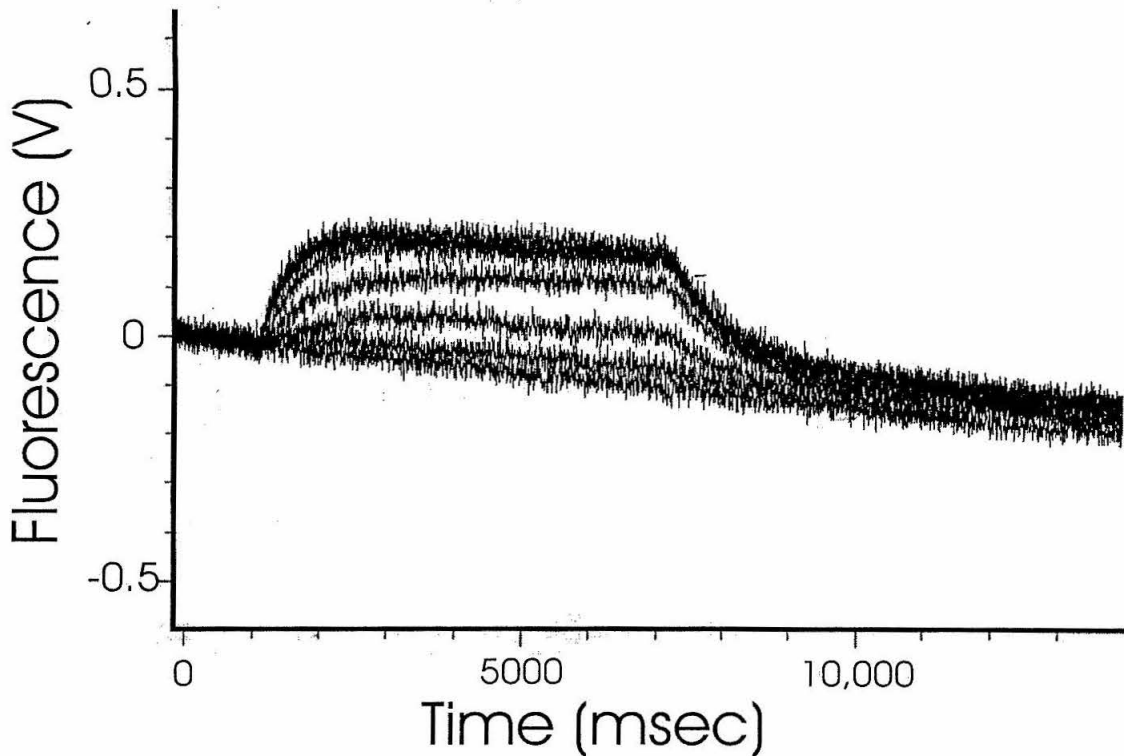


Figure 4.5 Slow upward ΔF from eYFP Δ C-FlaSh. Voltage recording and photometry show fluorescence changes in response to long voltage steps. Voltage steps (not shown) from -80 mV to $+20$ mV, in 20 mV increments. Holding potential was -80 mV. Note that ΔF from eYFP-FlaSh is very slow compared to FlaSh. For steps to $+20$ mV, $F_{on} = 420$ msec, $F_{off} = 720$ msec. Fluorescence scale, 2% .

We could not induce stereotyped fluorescence pulses from eYFP-Flash in response to short membrane depolarizations, as we could with FlaSh. The slow upward ΔF in eYFP-FlaSh required long depolarizations and the ΔF returned to baseline fluorescence (F_{off}) coincident with the repolarization of the membrane.

It is unclear why eYFP-FlaSh exhibits a slow upward ΔF in response to sustained depolarizations. It is interesting to note that eYFP is intrinsically more pH sensitive than wtGFP, eGFP, or eCFP. (Citation) One wonders whether the pH sensitivity of eYFP is related to the ΔF we see in eYFP-FlaSh. It is unlikely that the fluorescence change of eYFP-FlaSh is caused only by a pH artifact, because the size of the fluorescence change correlates with the gating charge movement in Shaker. Also, if the fluorescence change were caused by a pH change, we would expect the effect to reverse its sign at the proton "reversal

potential” of approximately -5 mV. The ΔF from eYFP-FlaSh increased monotonically (and sigmoidally) with increasing depolarization.

It would be interesting to introduce the mutations V68L / Q69K into eYFP-FlaSh. These mutations have been shown by (Miyawaki, Griesbeck et al. 1999) and others to reduce the pH-sensitivity of eYFP. One might predict that these mutations would alter, or even eliminate, the slow, upward ΔF we see in eYFP-Flash. These mutations might be help to explain the mechanism of the ΔF in eYFP-FlaSh. Additionally, a modified eYFP could simplify the fluorescence readout for FRET sensors based on eYFP-FlaSh/eCFP-FlaSh. (See next section.)

<i>GFP Variant</i>	<i>Optical Filter</i>	$\sim\Delta F_{max}$	<i>DIRECTION (~time constants)</i>
wtGFP Δ C (FlaSh)	HQGFP	$5.1 \pm 0.7\%$ (n=7)	DOWNWARD (~85 msec)
	HQFITC		DOWNWARD (~85 msec)
eGFP Δ C (F64L / S65T)	HQGFP	None	None
	HQFITC	$0.29 \pm 0.03\%$ (n=3)	DOWNWARD (too noisy)
ECFP Δ C (F64L / S65T / Y66W / N146I / M153T / V163A / N212K)	HQGFP	None	None
	HQFITC	None	None
eYFP Δ C (S65G / S72A / T203Y)	HQGFP	None	None
	HQFITC	$4.9 \pm 0.6\%$ (n=3)	UPWARD (420 msec - SLOW!)

Table 4.6. Fluorescence changes in FlaSh, FlaSh-eGFP, FlaSh-eCFP, FlaSh-eYFP. Maximal fluorescence changes are \pm SEM. Time constant is for voltage steps from -80 mV to $+0$ mV

Summary

Unfortunately, none of the eGFP-FlaSh, eCFP-FlaSh, or eYFP-FlaSh chimeric sensors responded to membrane depolarizations with a ΔF that was larger or faster than FlaSh. However, results from this work do suggest that protonation/deprotonation of the chromophore might be involved in the fluorescence change we see in FlaSh. In addition, FlaSh-eYFP and FlaSh-eCFP could be useful for making FRET sensors based on FlaSh. (See section that follows.)

Applications of FlaSh color variants

4.6 FlaSh sensors based on FRET

The maximal fluorescence change ($\Delta F/F$) in FlaSh is approximately 5%, ignoring the temporal amplification provided by FlaSh. By comparison, the $\Delta F/F$ for some membrane voltage organic dyes can be as high as 50% (González and Tsien 1997) and the $\Delta F/F$ for organic dyes used to measure intracellular calcium levels can be as high as 2000% (Tsien 1989). Clearly, it would be useful to improve the $\Delta F/F$ from FlaSh for the purpose of visualizing neural activity *in vivo*. We reasoned that fluorescence energy transfer (FRET) could be a rational tool for improving the response of FlaSh to membrane voltage.

As shown in previous chapters, wtGFP Δ C, eYFP Δ C, and eCFP Δ C can be inserted into a variety of locations in the Shaker channel. One approach to improving the response of FlaSh would be to look for other locations in Shaker where GFP can be inserted. Another approach would be to increase the sensitivity of GFP to its environment, e.g. to pH or to ionic strength, and to create FlaSh sensors based on a sensitized GFP. (For a discussion of this approach, see the combinatorial methods outlined in the last chapter.) We believed that FRET could provide a rational mechanism for improving the signal from FlaSh. Therefore, we constructed and tested a variety of eYFP-FlaSh and eCFP-FlaSh chimeras and tested them by co-injection in oocytes.

4.7 Constructing eYFP-FlaSh and eCFP-FlaSh sensors for FRET

One possibility would have been to insert both eYFP and eCFP into a single Shaker subunit at a variety of locations. However, this would have been time consuming. Because it is known that the Shaker channel functions as a tetramer (Isacoff, Jan et al. 1990), we chose instead to design sensors where FRET occurs between eCFP and eYFP located on different subunits of the Shaker channel. This approach enabled us to test a larger range of location pairs. For example, for N locations in Shaker, we had only to make $2N$ constructs and test them by mRNA co-injection. By comparison, it would have required $N \times N = N^2$ constructs to test dual-GFP monomers.

We used mutagenesis coupled PCR to insert eYFP Δ C and eCFP Δ C into several locations in Shaker. These locations are shown in figure 4.7. Note that we tested only a subset of the 36 possible 1:1 co-injections, and these measurements are indicated in the figure by heavy red lines. Based on our knowledge of Shaker, we chose locations that we believed might undergo movements relative to one another during gating, inactivation, or slow inactivation of the channel.

All measurements were done in the *W434F* background, which abolishes ionic current through the channel. Fluorescence measurements were done in *Xenopus* oocytes by exciting eCFP with short wavelength light (440 – 480 nm) and measuring short wavelength (longpass, dichroic) emission from eCFP or long wavelength (505 nm longpass, dichroic) emission from eYFP, using a fluorescence filter cube and voltage clamp fluorimetry. Results were repeated for each oocyte ($n \geq 2$ for each co-injection). The qualitative results of these co-injection experiments are discussed below.

N-terminal-eYFP (#1) FlaSh co-injection with {#1, #2, #4, #5, #6}

We co-injected N-terminal-eYFP-FlaSh with N-terminal-eCFP-FlaSh (1), T1-eCFP-Flash (2), S6-eCFP-FlaSh (4), eCFP-FlaSh (5), or C-terminal-eCFP-FlaSh (6). All of these constructs produced functional channels, as measured by fluorescence and gating currents. We excited eCFP with short wavelength light. However, we did not see any correlation between electrical gating currents and the fluorescence emission of eCFP or eYFP. We had hoped that the fluorescence of these proteins might be sensitive to fast-inactivation of Shaker because of the proximity of eYFP Δ C to the fast-inactivation “ball” (Bezanilla, Perozo et al. 1991).

T1-eYFP (#2) FlaSh co-injection with {#2, #5, #6}

We co-injected T1-eYFP-FlaSh with T1-eCFP-Flash (2), eCFP-FlaSh (5), or C-terminal-eCFP-FlaSh (6). All of these constructs produced functional channels, as measured by fluorescence and gating currents. We excited eCFP with short wavelength light. We did not see any correlation between gating currents and the fluorescence emission of eCFP or eYFP.

eYFP-FlaSh (#5) co-injection with {#1, #2, #4, #5, #6}

We co-injected eYFP-FlaSh with N-terminal-eCFP-FlaSh (1), T1-eCFP-Flash (2), S6-eCFP-FlaSh (4), eCFP-FlaSh (5), and C-terminal-eCFP-FlaSh (6). All of these constructs produced functional channels, as measured by fluorescence and gating currents. We excited eCFP with short wavelength light.

In co-injections #5/#4 and #5/#5, we measured a reversible decrease in eYFP fluorescence in response to membrane depolarization. A representative trace from #5/#5 is shown in Figure 4.8. The $\Delta F/F$ of the response from eYFP was approximately 2%. We saw a coincident decrease in eCFP fluorescence of approximately 1.5%. The fluorescence change was sigmoidally related to voltage and followed the gating charge movement of the channel, as it does for FlaSh. We conducted parallel control experiments to verify that neither #4 nor #5 produced a fluorescence change when injected as a monomer. The response from #5/#4 was qualitatively similar in size and kinetics to #5/#5.

We did not see any correlation between gating currents and the fluorescence emission of eCFP or eYFP for any other eYFP-FlaSh (#5) co-injection.

C-terminal-eYFP (#6) FlaSh co-injection with {#1, #6}

We co-injected C-terminal-eYFP-FlaSh with N-terminal-eCFP-FlaSh (1), or C-terminal-eCFP-FlaSh (6). All of these constructs produced functional channels, as measured by fluorescence and gating currents. We excited eCFP with short wavelength light. However, we did not see any correlation between electrical gating currents and the fluorescence emission of eCFP or eYFP.

FlaSh sensors based on FRET

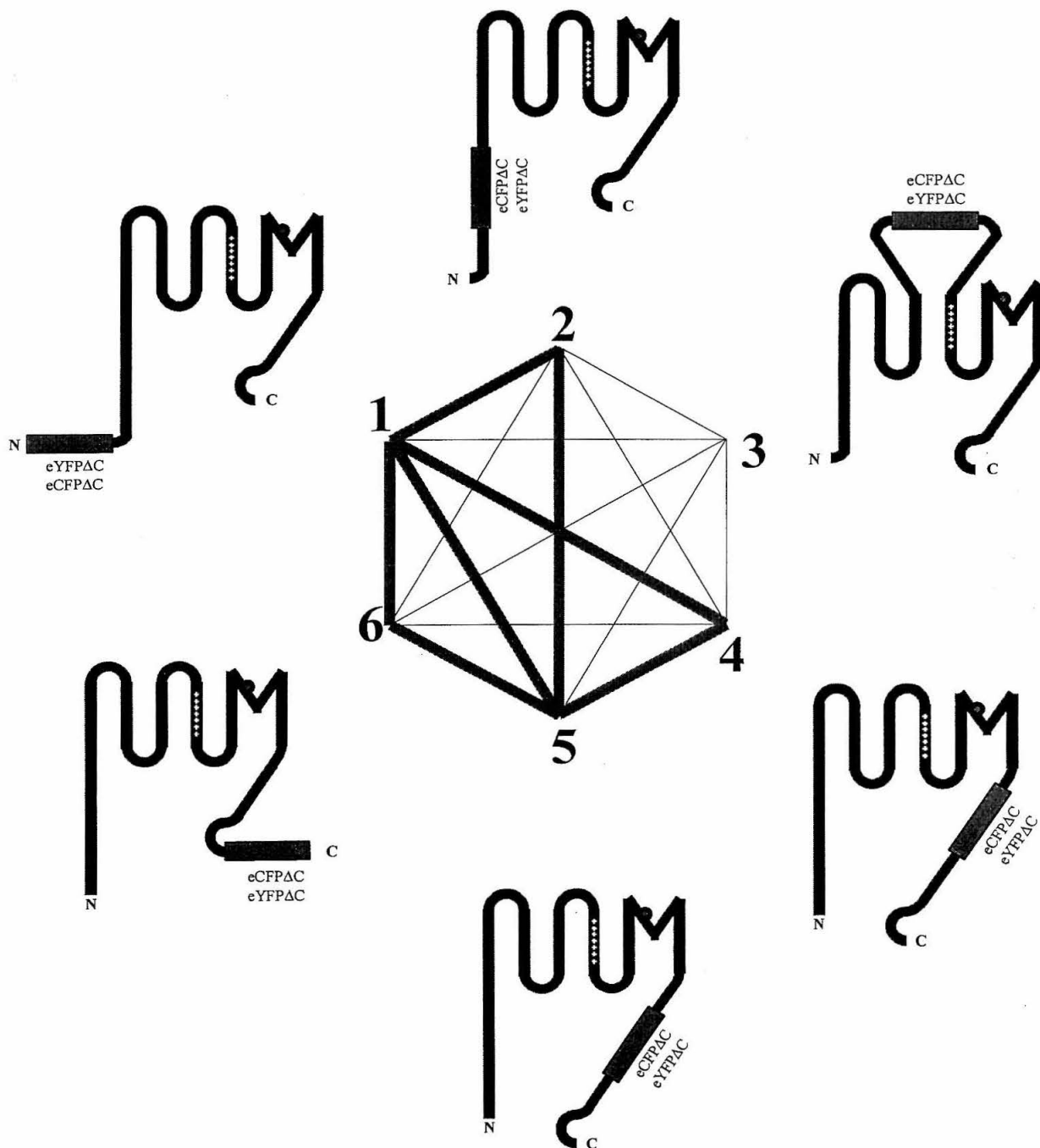


Figure 4.7 FRET between eCFP Δ C-FlaSh and eYFP Δ C-FlaSh. Co-injection between differently colored FlaSh monomers, which co-assemble in 1:1 molar ratio. Thick red lines indicate those co-injections that we tested in oocytes. Our selection was based on intuition from structural studies of Shaker. See text.

Figure 4.8 FlaSh-eCFP/eYFP FRET. Fluorescence output from FlaSh-eCFP (#5) and Flash-eYFP (#5) co-injections. Excitation (nm) excited eCFP via short wavelength light; we measured emission from eCFP (nm) and eYFP (nm) during voltage steps from -80 mV to $+20$ mV. Notice coincident upward ΔF from eYFP and downward ΔF from eCFP. Time constants $F_{on}=23$ msec, $F_{off}=105$ msec. Scale bar, 2%

	1	2	3	4	5	6
1	*				*	*
2	*	*			*	
3						
4	*				Y \uparrow 2%; C \downarrow 1.5%	
5	*	*			Y \uparrow 2%; C \downarrow 1.5%	
6	*	*			*	*

Table 4.9 FlaSh-eCFP/eYFP FRET. Pairwise co-injection between eYFP (horizontal) and eCFP (vertical) Shaker constructs. eYFP or eCFP was inserted into location corresponding to figure 4.7. * indicates functional channel expression but no ΔF . Note that no constructs were tested at location 3 because GFP insertion at this location interrupts channel function.

Summary

We engineered FlaSh sensors that use FRET between eYFP and eCFP on different subunits of Shaker. The results of this work is shown in table 4.9. Although the $\Delta F/F$ of approximately 2% is smaller than the original FlaSh, it is reasonable that this figure could be improved by tuning the locations of eYFP or eCFP within Shaker.

FRET-based sensors have the additional advantage that their output is intrinsically ratiometric (Tsien 1989). A ratiometric output is advantageous *in vivo*, because the ratio between two fluorescent signals is robust to differences in fluorophore concentration and motion artifacts. (See Chapter 6.) It would be interesting to place eCFP or eYFP comprehensively through the region between S6 and the endogenous Spe I site in Shaker, as a way of improving the $\Delta F/F$ of the FlaSh sensor. Alternatively, one could imagine the advantages of a combinatorial approach, such as those discussed in Chapter 7, to generate and screen functional libraries of eCFP/eYFP FlaSh sensors.

If one finds locations in Shaker that produce a larger $\Delta F/F$ from eCFP/eYFP, it would be interesting to explore whether eCFP and eYFP could be introduced into a single monomer Shaker. Alternatively, one could attempt to make tandem dimer constructs, as discussed in Chapter 3.

Finally, the fluorescence change we see from eYFP-Flash (#5) / eCFP-FlaSh (#5) co-injections could give some insight into the fluorescence change we see in FlaSh. In FlaSh, four GFPs are presumably packed closely together around Shaker. A change in FRET efficiency between eCFP-FlaSh and eYFP-FlaSh suggests that, during the fluorescence change in FlaSh, there is a change in the distance or mutual orientation between these four GFP modules.

Chapter 5

G protein-coupled FlaSh

In the previous chapters we described FlaSh, a genetically encoded sensor that measures membrane voltage. FlaSh is a chimeric protein between the Shaker K⁺ channel and GFP. We showed that the fluorescence of GFP in FlaSh is dependent on structural rearrangements involved in gating and inactivation of the Shaker channel and that mutations in Shaker predictably alter the behavior of FlaSh.

In this chapter, we will discuss our preliminary efforts toward a fluorescent sensor based on a G-protein activated Inwardly Rectifying K⁺ channel (Girk 3.3). We chose Girk3.3 because it is homologous to Shaker but its activation is dependent on intracellular g-protein second messengers. We will explain the motivation for building a fluorescent sensor for G-protein signaling. Then we will outline our initial experiments and describe the functional effect of fusing wtGFP, eYFP, and eCFP into various regions of Girk3.3.

5.1 G protein-coupled receptors as therapeutic targets

We designed FlaSh to visualize electrical activity arising from networks of neurons *in vivo*. By contrast, our motivation for the sensor described in this chapter is to measure signal transduction events in single cells *in vitro*. In particular, we were interested in building fast, accurate assays of receptor activation. As part of their drug discovery efforts, the pharmaceutical industry screens libraries of potential therapeutics against receptor targets in single cells. We thought that a fluorescent sensor like FlaSh, but sensitive to more general measures of cell signaling, could be valuable for this purpose.

G-protein coupled receptors (GPCRs) are a superfamily of integral plasma membrane proteins involved in a broad array of signaling pathways. Novel members of the GPCR superfamily have emerged through cloning activity as well as through bioinformatic analyses of sequence databases, although their ligands are unidentified and their physiological relevance remain to be defined. These “orphan” receptors provide a rich source of potential targets for drug discovery (Stadel, Wilson et al. 1997).

For example, within the last twenty years, several hundred new drugs have been registered that are directed towards activating or antagonizing GPCRs; it is estimated that most current research within the

pharmaceutical industry is focused on this signaling pathway (Roush 1996; Stadel, Wilson et al. 1997). Widely used drugs that target GPCRs include Morphine, Haldol, Seldane, Tagamet, and Zantac. The last two alone comprise a multi-billion dollar market for the treatment of ulcers.

GPCRs form one of the largest protein families found in nature, and it is estimated that approximately 1000 different receptors exist in mammals. Functionally, GPCRs share in common the property that upon agonist binding they transmit signals across the plasma membrane through an interaction with heterotrimeric G proteins (Neer 1995). However, the diversity of receptors appear to interact with only a limited repertoire of G proteins. (Reviewed in (Gudermann, Kalkbrenner et al. 1996).)

We wanted to design a fluorescent sensor that could reflect activity from a diverse range of receptors. At the same time, we wanted the sensor to be specific for receptor activation, and not to be confounded by other responses in the cell.

Our idea was that a sensor for G protein activity could be both modular and generic: the sensor could be introduced into a stable cell line, along with the receptor of interest, and whole-cell fluorescence would indicate the activity of the receptor. A G protein sensor could be useful, 1. to screen a chemical library against orphan GPCRs, or 2. to optimize an existing drug, such as morphine, that interacts with a known GPCR, such as the μ -opioid receptor.

A generic sensor: G proteins as proxy for GPCR activation

A diverse range of GPCRs are known couple to a diverse range of intracellular effectors through a limited repertoire of G proteins. In this way, the cell can react to a multitude of chemical signals (e.g, hormones, neurotransmitters, growth factors, and odorants); and an individual chemical signal can induce a multitude of physiological changes inside the cell (e.g., by modulating enzymes, transporters, and ion channels). Because information about the extracellular environment is funneled through G proteins, one idea is to detect the activation of intracellular G-proteins as a proxy for receptor activation. In this way, the sensor could be used in principle with a variety of GPCRs, including “orphan” receptors with unknown function.

An outline of our approach appears in figure 5.1. We chose to use the μ -opioid receptor, which couples to GIRK3.1.

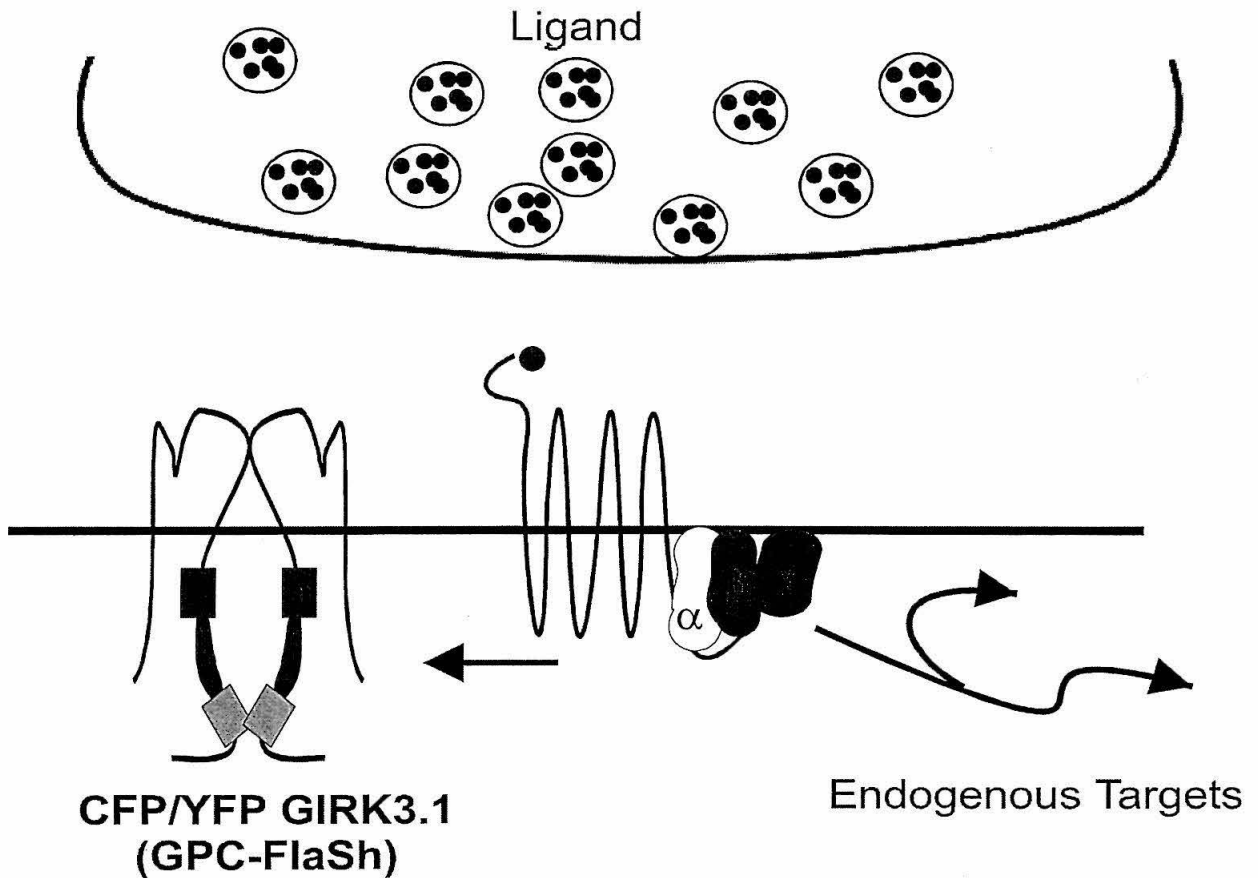


Figure 5.1. G Protein Coupled FlaSh. Extracellular signals (e.g., neurotransmitter) activate G protein coupled receptor, causing G protein beta-gamma subunits to dissociate from G protein alpha subunit. Free beta-gamma dimers stimulate a wide variety of intracellular targets, including ion channels like GIRK 3.1. GPC-FlaSh is based on GIRK3.1, an inwardly rectifying K⁺ channel that is homologous to Shaker K⁺ channel.

5.2 Inwardly rectifying potassium channels

The study of “anomalous rectification” has a rich history that dates back fifty years to Katz (Katz 1949; Doupnik, Davidson et al. 1995). Many electrically active cells possess inwardly rectifying K⁺ (Kir) channels through which current flows more easily in the inward direction than outward. (Reviewed in (Doupnik, Davidson et al. 1995; Shojiro, Kondo et al. 1997)). The inwardly rectifying potassium channels exhibit rectification in that they pass current preferentially in the inward direction. This current has been termed anomalous because it is opposite to the voltage-dependent delayed K⁺ current in the squid giant axon (Hodgkin, Huxley et al. 1952).

Recent evidence has shown that DNAs encoding Kir channels contain two putative transmembrane domains and a pore forming region. These regions are homologous to the fifth and sixth transmembrane regions, and to the pore region of Shaker and other voltage-dependent (Kv) channels. Based on their homology to Shaker, we thought Kir could make a good backbone for a fluorescent sensor.

Kir3, a subfamily of inwardly rectifying potassium channels, are activated by G proteins. In mammals, Kir3 is known to be expressed: in the heart (where cholinergic stimulation helps to slow the heartbeat), in the brain (where they suppress neuronal firing), and in the pancreas (where they are involved in insulin secretion). We chose to work with Kir3.1 (Girk 3.1) (Dascal, Schreibmayer et al. 1993; Kubo, Reuveny et al. 1993), which is known to couple to the μ -opioid receptor. This was coinjected with Kir3.4 (also known as: rckATP) (Ashford, Bond et al. 1994). Coinjection with rckATP is known to increase functional expression of Kir3.1 in oocytes.

5.3 GFP insertion locations in Girk3.1

We inserted wtGFP Δ C, eYFP Δ C, eCFP Δ C in a variety of locations in Girk3.1, as shown in figure 5.2. Note that M1, M2, and H5 regions of Girk3.1 are homologous to the S5, S6 transmembrane regions and to the pore of Shaker, respectively. Therefore, we reasoned that it might be interesting to place GFP after M2, near where we placed GFP in FlaSh.

We chose three locations {5,6,7} just after M2 in Girk3.1 and used mutagenesis coupled PCR to insert wtGFP Δ C. Figure 5.3 shows the physiological response of these chimeric sensors, as compared to

the wild type channel. Note that GFP inserted into Girk3.1 at locations 5 and 7 appear to render the channel non-functional. However, Girk3.1 with GFP inserted into location 6 does respond to intracellular G protein stimulation (via DAMGO coupling through the μ -opioid receptor).

Likewise, we inserted GFP Δ C into locations near the putative binding sites for G protein beta-gamma subunits. (reference) As shown in figure 5.3, Girk3.1 with GFP inserted into locations 6 and 9 also respond to intracellular G protein stimulation.

We saw fluorescence above background from {4,6,9}-GFP-Girk3.1. However, under epi-illumination and voltage-clamp fluorimetry, we could not measure any ΔF in response to agonist or voltage for these channels. Note these oocytes were **not** as bright as oocytes expressing FlaSh; presumably this is because the oocytes are unable to express conducting K⁺ channels at high levels.

It is interesting that the total channel expression for the chimeric proteins is in every case lower than the wild type Girk3.1. However, at least for locations 4 and 9, the relative size of the induced current is larger than it is in the wild type channel. This could indicate that in the chimeric proteins GFP interferes with the binding of G protein beta-gamma subunits to Girk3.1. If this is the case, one might expect that the induced current should activate slower than the wildtype current.

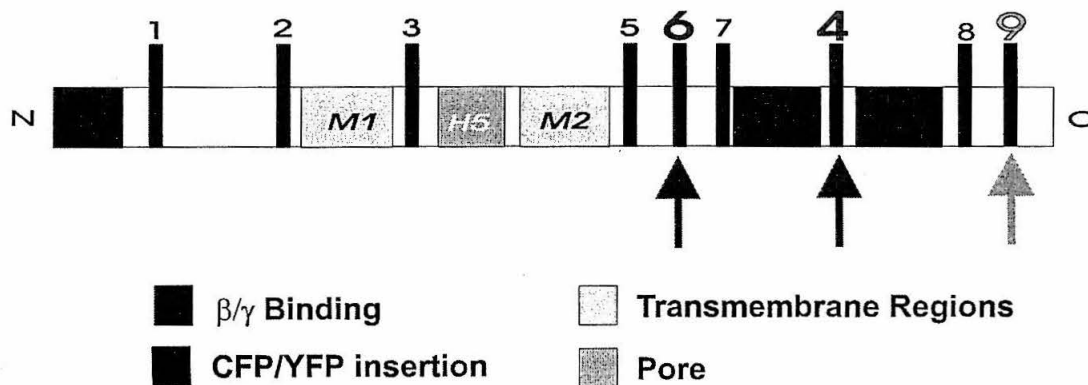


Figure 5.2. GFP insertion into G-protein coupled K⁺ channel. We inserted wtGFP Δ C, eYFP Δ C, and eCFP Δ C into nine locations in Girk3.1. M1 and M2 transmembrane regions of Girk are shown, along with pore. These regions are homologous to the fifth and sixth transmembrane regions and the pore of Shaker. Note three putative G protein beta-gamma binding domains.

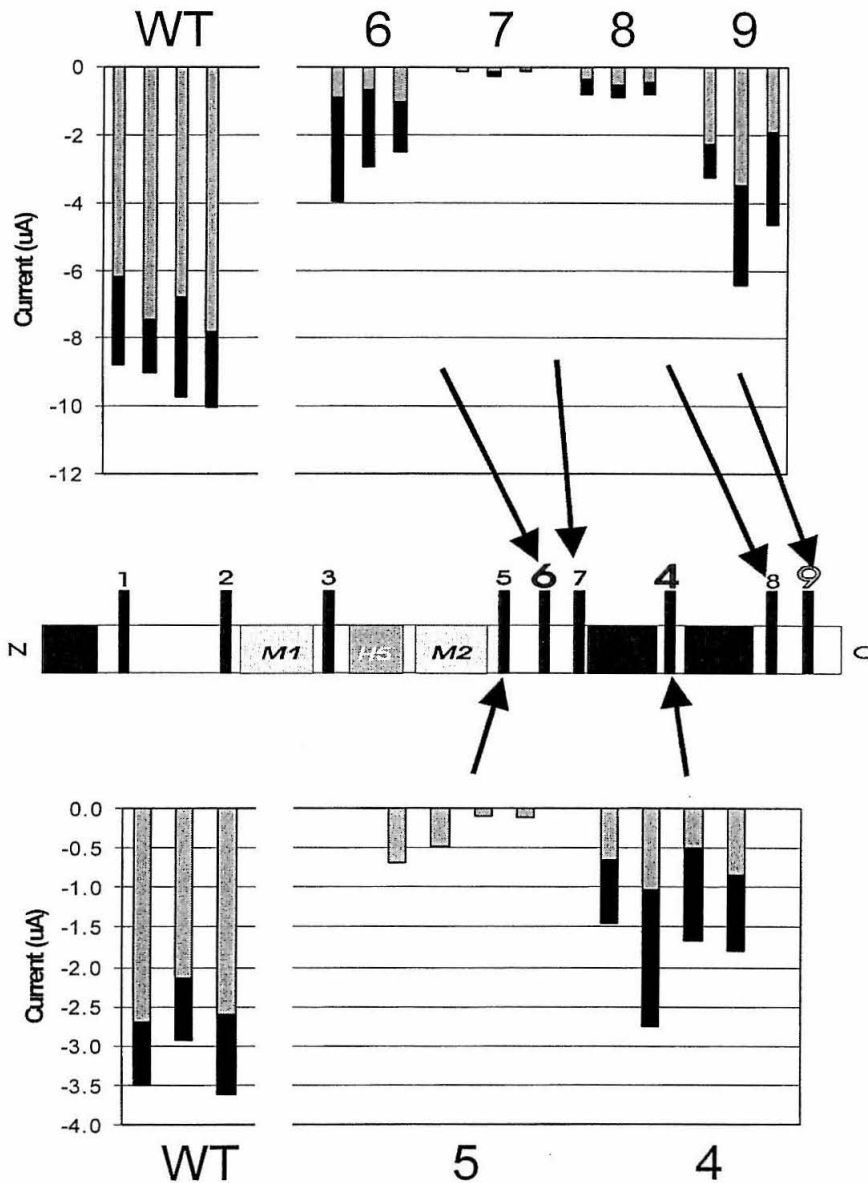


Figure 5.3. Physiological response of Girk3.1-wtGFP. We measured basal current (grey) and agonist-induced current (black) for six GFP insertion locations in Girk3.1. Response of WTGirk3.1 is shown for comparison. Note response from locations {4,6,8,9}. mRNA was co-injected 1:1:1 with rckATP (Girk 3.4) and μ -opioid receptor and stimulated with 200nM DAMGO. Each vertical measurement is response from one oocyte. {6,7,8,9} were performed one oocyte batch; {4,5} were performed on another oocyte batch.

5.4 eYFP/eCFP-Girk3.1 is slower than wtGirk 3.1.

By analogy to FlaSh, we thought it might be possible to generate a FRET sensor based on Girk3.1 using eCFP and eYFP. As a preliminary effort toward this end, we inserted eYFP into location 9 and eCFP into location 4 into Girk3.1.

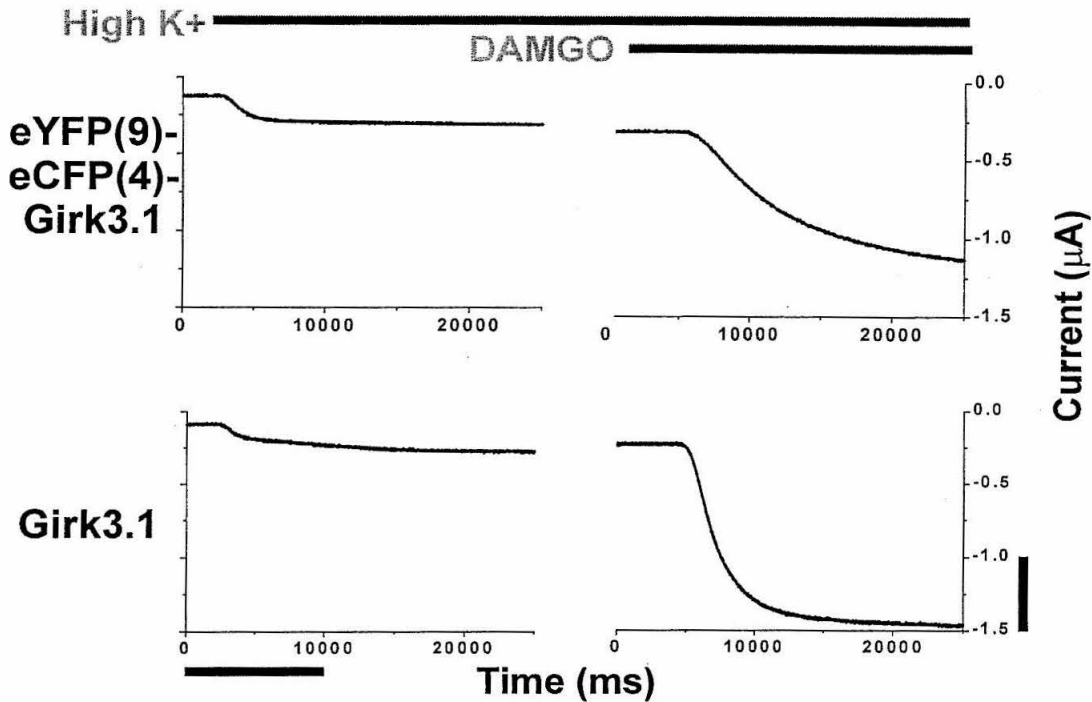


Figure 5.4. Physiological response of Girk3.1 and eYFP-eCFP-Girk3.1. We introduced both eYFP (9) and eCFP (4) into Girk3.1, in locations shown in figure 5.2. Electrical current measured continuously in low K⁺ (2mM), high K⁺ (96mM), and then high K⁺ with DAMGO (96mM K⁺, 200 nM DAMGO). Note that a fraction of the channels are endogenously open. However, both wtGIRK and eCFP-eYFP-GIRK respond to the DAMGO. mRNA was co-injected 1:1:1 with rckATP (Girk 3.4) and μ -opioid receptor. Scale, 0.5 μ A, 10 sec.

We measured basal currents and currents induced by DAMGO, as above. We chose locations 4 and 9 because Girk3.1 with single GFP inserted into 4 and 9 retained basal and agonist-induced currents. (See Figure 5.3.) We were unable to measure any change in fluorescence in response to DAMGO in the double insertions. However, it is remarkable that with two GFP insertions the channel retained basal and agonist induced currents, as shown in Figure 5.4. Note that the agonist-induced current is slower in Girk3.1/eCFP(4)/eYFP(9) double insertion than it is in wt Girk3.1. This is consistent with the model that GFP inserted into location 4 or location 9 interferes with the binding of G protein beta-gamma subunits to Girk3.1.

Chapter 6

Future Directions

In this thesis we have described several genetically encoded optical sensors that measure cell signaling cascades. In general, the design of these sensors has benefited from structural knowledge about signal transduction proteins; in the case of FlaSh, structure/function studies on the Shaker potassium channel guided our intuition and inspired the design of various chimeric proteins. In addition, information about the Shaker channel guided our attempts to create chimeric sensors based on homologous channels, e.g., HERG and GIRK.

The approach taken in this thesis has been rational and serial: we designed several sensors, constructed them in separate reactions, and tested each sensor in oocytes to check for function. This approach was reasonably successful for sensors based on Shaker and its homologues. However, it is useful to discuss another approach that could have been used and might prove to be useful in other situations.

In many areas of molecular biology, it has been possible to optimize a protein of interest by generating large libraries of mutant proteins and screening for those which are improved in some aspect. This general approach has been called evolutionary, random, or irrational optimization. Random methods have been used widely, e.g., to improve the function of an enzyme (Cramer, Raillard et al. 1998), the fluorescence of GFP (Cramer, Whitehorn et al. 1996), or the binding affinity of a peptide to a therapeutic target *in vivo* (reviewed in (Cesareni, Castagnoli et al. 1999)).

In the sections that follow we will discuss two applications of random protein optimization and suggest ways in which this technique could be used to generate chimeric protein sensors.

6.1 Sensitizing GFP to pH with random optimization

Miesenbock et al. (Miesenböck, De Angelis et al. 1998) describe GFP-based sensors of secretion and neurotransmission in living cells. Their idea follows from the knowledge that the pH inside the vesicle is largely acidic, whereas the pH outside the cell is neutral. Therefore, the pH sensitivity of a vesicle-attached fluorescent protein could be used to monitor vesicle exocytosis. (For another approach to this

problem, see chapter 6, section 6.2.) The fluorescence of wildtype GFP is essentially unaltered between pH 5.5 and pH 10, which makes it non-optimal as a sensor of vesicle exocytosis. However, Miesenbock et al. were able to improve on the pH-sensitivity of GFP by applying a random method.

Using directed random PCR-mutagenesis, Miesenbock et al. randomized five regions that are known from the crystal structure of GFP to be involved in the proton-relay network of GFP (Brejc, Sixma et al. 1997). Presumably, this proton-relay network is one mechanism by which external pH can modulate the fluorescence of GFP.

Miesenbock et al. cloned and amplified this GFP library in bacteria and examined over 19,000 separate mutant fluorescent proteins. Technically, this required screening over two hundred 96-well plates containing bacteria expressing members of the library (!). By comparing fluorescence in these clones in conditions of both high pH and low pH, Miesenbock et al. were able to isolate several mutant GFPs that had the property that they were exceptionally sensitive to pH.

One of these mutants, termed “ecliptic pHluorin,” exhibits large changes in fluorescence over the requisite pH range, when excited with 470nm light. Ecliptic pHluorin is fluorescent at pH 7.5, but it is non-fluorescent at pH < 6. This is a significant improvement over the wildtype GFP. Miesenbock et al. successfully transfected this construct into single cells and used it to measure vesicle secretion in single cells.

6.2 Improving GFP fluorescence with evolutionary PCR

The fluorescent sensors described in this thesis have been generated through mutagenesis coupled PCR, which is rational and serial. As discussed above, Miesenbock et al. used PCR-cassette mutagenesis to improve the pH sensitivity of GFP. However, similar to mutagenesis coupled PCR, the approach of Miesenbock et al. was informed by knowledge of the structure of GFP determined by X-ray crystallography.

(Cramer, Whitehorn et al. 1996) provides a radical departure from these approaches. Cramer et al use the technique of molecular evolution by DNA shuffling to improve the fluorescence intensity of GFP. Their brightest mutants are improved 42-fold over the wildtype GFP sequence, as measured by

simple emission intensity when excited by 365nm light. An interesting feature of DNA shuffling (Cramer, Whitehorn et al. 1996) is that it can be used with no knowledge of the structure of the target protein. In this case, the technique enabled Cramer et al. to improve the fluorescence of GFP without understanding the mechanism by which GFP is fluorescent.

Mutagenizing a protein by DNA shuffling involves: first, amplifying the protein using PCR under conditions where DNA polymerase introduces point mutations; second, shattering this library into small DNA fragments; third, allowing the fragments to assemble into full-length genes via self-priming. The process yields crossovers between mutations due to PCR template switching. Coupled with a functional screen (e.g., fluorescence intensity), and through a process of iteration, this procedure allows recombination between positive mutations while simultaneously removing negative mutations from the sequence pool.

There is at least one significant challenge when optimizing a protein by random methods, and this is to design an effective screening assay. Fluorescence intensity is a particularly simple assay. It is significantly more challenging to measure a multiplicity of clones for increased pH sensitivity, Ca^{++} sensitivity, or sensitivity to a small peptide.

In general, it is also difficult to design an assay that selects for the desired feature without also selecting for unintended (possibly undesirable) features of the protein. For example, the 42-fold increase in fluorescence intensity ascribed to the mutant GFP of Cramer et al. is due partly to an increase in protein solubility. When expressed at high levels in bacteria, wildtype GFP is mostly insoluble in the form of inclusion bodies; whereas, the mutant GFP discovered by Cramer et al is mostly soluble and was more likely to activate its chromophore.

DNA shuffling is technically simple in bacteria. Therefore, Cramer et al optimized the whole cell fluorescence signal in bacteria, and assayed the performance of the best GFP mutants in eukaryotic cells. This indicates another potential problem with DNA shuffling. It is difficult to express many kinds of membrane-bound proteins like Shaker in bacteria. Therefore, it might be useful to develop methods for DNA shuffling directly in eukaryotic cells. Creating DNA libraries in eukaryotic cells is limited partly by the low transformation efficiency of eukaryotic cells relative to bacteria. Low transformation efficiency limits the size of the mutant library that can be tested.

6.3 Conclusion

This project began with a challenge to visualize electrical activity in living tissue. We discussed the difficulty in this problem: cells can be small ($<5\ \mu\text{m}$), and action potentials can be short ($<5\ \text{msec}$). For example, it is estimated that $1\ \mu\text{l}$ of cerebral cortex contains one million (1,000,000) neurons and one billion (1,000,000,000) synapses.

In this thesis, we have described a different approach to the problem of imaging living tissue. We asked the question: how can one induce the tissue to synthesize a probe from the inside? This approach required us to design a novel gene whose protein product, when expressed in living tissue, produces a functional fluorescent sensor.

As described in chapter 2, we combined the genes for two distinct proteins to create a functional chimeric sensor called FlaSh. We used the Shaker potassium channel, which has been designed by nature to measure and to respond to individual action potentials; and we used the green fluorescent protein (GFP), from the jellyfish *Aequorea victoria* to create a fluorescence readout. FlaSh produces a fluorescent signal that is triggered by individual electrical events in living cells.

In chapter 3, we described various precursors to FlaSh. For example, we enumerated some chimeric proteins that did not produce functional sensors. We also described modifications to FlaSh that change its color, its kinetics, and improve its dynamic range.

In chapter 4, we described various attempts to improve FlaSh by using fluorescence resonance energy transfer, which is a physical effect whereby two fluorescent molecules can interact in a manner that is dependent on their distance and mutual orientation. We described sensors that contain multiple copies of GFP and that produce a ratiometric fluorescence output. In principle, these sensors have the advantage that they can be improved by rational or semi-rational genetic manipulations.

In chapter 5, we discussed initial work toward a more generalized sensor of cellular activity. In particular, we described ratiometric fluorescence sensors designed to respond to G-protein coupled receptor (GPCR) activation. When successful, these sensors will have unique commercial applications in the area of high-throughput drug screening.

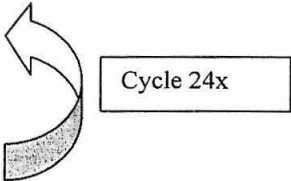
Finally, in this chapter, we summarized future directions for this work. The field of genetically encoded physiological sensors is subtle and largely unexplored. The initial efforts described in this thesis

will have been most successful if we can inspire others to improve on their design and to use them in living tissue.

Appendix A – Experimental Procedures

Construction of the FlaSh Membrane Probe and Its Homologues

We amplified GFP Δ C from the plasmid TU#65 (Chalfie, Tu et al. 1994) using the polymerase chain reaction with primer sequences CCACTAGTAAAGGAGAAGAAGCTTTTC and GGACTAGTGCCATGTGTAATCCCAGCAGCTGT. In the case of wtGFP, eGFP, eCFP, and eYFP, we used the following PCR protocol to amplify green fluorescent protein for mutagenesis-coupled-PCR:

1. 94°C for 2 minutes
 2. 94°C for 1 minute
 3. 50°C for 1 minute
 4. 72°C for 1 minute
 5. 72°C for 7 minutes
- 

The primers listed above amplify amino acids 2-233 of GFP and add SpeI restriction sites in-frame to both ends. *ShH4* (gift of Liga Toro) had been cloned into pBluescript (Stratagene), and site-directed mutagenesis was used to engineer the point mutation *W434F*, which blocks ionic current through the channel. GFP Δ C was inserted into *ShH4-W434F* at the SpeI restriction site by using standard techniques (Sambrook, Fritsch et al. 1989), and the orientation of the insert was verified by digesting with NcoI, which cuts asymmetrically in GFP Δ C and *ShH4*. We also digested with HpaI to verify that only a single copy of GFP Δ C was inserted into *ShH4-W434F*. The FlaSh cDNA was transcribed using Megascript T7 (Ambion, Austin, TX) with a 4:1 methyl CAP to rGTP ratio, and the precipitated cRNA was resuspended in ultrapure water (Specialty Media, Laballete, NJ) for injection.

Voltage-Clamp Fluorimetry

Oocyte isolation, injection, and incubation were as described previously (Isacoff, Jan et al. 1990). Two-electrode voltage clamping was performed with a Dagan CA-1 amplifier (Dagan Corporation,

Minneapolis, MN). External solution was NaMES (110 mM NaMES, 2mM CA[MES]₂, and 10 mM HEPES [pH 7.5]). Capacitance compensation was performed from a holding potential of 60 mV. An HC120-05 photomultiplier (Hamamatsu, Bridgewater, NJ) was used for fluorescence measurements, on a Nikon TMD inverted microscope.

Data was sampled at 4 kHz and fluorescence signals were low-pass filtered at 1 kHz with an 80pole bessel filter (Frequency Devices, Haverhill, MA). Data was acquired onto a Digidata 1200 A/D interface (Axon Instruments, Foster City, CA). Data acquisition and analysis were done with Axon Instruments PClamp 6. Illumination was with a 100 W Hg Arc lamp. When measuring from the wildtype FlaSh, exciting and emitted light were filtered through an HQ-GFP filter (Chroma Technology, Brattleboro, VT), with the following bandpass: excitation filter, 425-475 nm; dichroic, 480 nm long-pass; emission filter, 485-535 nm.

G-protein Coupled Receptors and Ligand Perfusion

We amplified GFP Δ C using the same protocol as above. We eliminated an endogenous SpeI site in our pBSIIks+ GIRK3.1. Following this, we used site-directed mutagenesis as above to introduce a unique SpeI site in GIRK. These experiments were done as a co-injection with GIRK-GFP Δ C, rckATP (also called GIRK3.4), and μ -opioid receptor. cRNA was transcribed using Megascript T7 (Ambion, Austin, TX) with a 4:1 methyl CAP to rGTP ratio, and the precipitated cRNA was resuspended in ultrapure water (Specialty Media, Laballete, NJ) for injection.

Co-injection ratios were standard, as described in (Ashford, Bond et al. 1994). Perfusion in single oocytes was done using gravity flow. Two-electrode voltage-clamp and fluorescence measurements were as described above.

Analysis

Oocyte isolation, injection, and incubation were as described previously (Isacoff, Jan et al. 1990). Charge-voltage relations were constructed from the integrated off gating currents, evoked by repolarizations to -80 mV, after depolarizations that were long enough for the on gating current to decay to

completion. Fluorescence-voltage relations were constructed from the amplitudes of the “on” fluorescence change from steps long enough to reach steady state. Some fluorescence traces in Chapter 2 were digitally RC filtered at 300 Hz. Linear reconstructions in chapter 2 were performed with Matlab software (MathWorks).

Confocal images were acquired on a Nikon PCM-2000 microscope using the 488 nm line of an Argon laser. Images were analyzed using the public domain NIH Image program (developed at the U.S. National Institutes of Health).

References

- Amsterdam, A., S. Lin, et al. (1995). "The *Aequorea victoria* green fluorescent protein can be used as a reporter in live zebrafish embryos." *Developmental Biology* **171**(1): 123-9.
- Ashford, M. L. J., C. T. Bond, et al. (1994). "Cloning and functional expression of a rat heart Katp channel." *Nature* **370**: 456-59.
- Baird, G. S., D. A. Zacharias, et al. (1999). "Circular permutation and receptor insertion within green fluorescent proteins." *Proceedings of the National Academy of Sciences of the United States of America* **96**(20): 11241-6.
- Baukrowitz, T. and G. Yellen (1995). "Modulation of K⁺ current by frequency and external [K⁺]: a tale of two inactivation mechanisms." *Neuron* **15**(4): 951-60.
- Baumann, A., A. Grupe, et al. (1988). "Structure of the voltage-dependent potassium channel is highly conserved from *Drosophila* to vertebrate central nervous systems." *Embo Journal* **7**(8): 2457-63.
- Bezanilla, F., E. Perozo, et al. (1991). "Molecular basis of gating charge immobilization in Shaker potassium channels." *Science* **254**(5032): 679-83.
- Brejci, K., T. K. Sixma, et al. (1997). "Structural basis for dual excitation and photoisomerization of the *Aequorea victoria* green fluorescent protein." *Proceedings of the National Academy of Sciences of the United States of America* **94**(6): 2306-11.
- Callahan, C. A. and J. B. Thomas (1994). "Tau-beta-galactosidase, an axon-targeted fusion protein." *Proceedings of the National Academy of Sciences of the United States of America* **91**(13): 5972-6.
- Cesareni, G., L. Castagnoli, et al. (1999). "Phage displayed peptide libraries." *Comb Chem High Throughput Screen* **2**(1): 1-17.
- Chalfie, M., Y. Tu, et al. (1994). "Green fluorescent protein as a marker for gene expression." *Science* **263**(5148): 802-5.
- Christie, M. J., R. A. North, et al. (1990). "Heteropolymeric potassium channels expressed in *Xenopus* oocytes from cloned subunits." *Neuron* **4**(3): 405-11.
- Clark, I., E. Giniger, et al. (1994). "Transient posterior localization of a kinesin fusion protein reflects anteroposterior polarity of the *Drosophila* oocyte." *Current Biology* **4**(4): 289-300.

- Cohen, L. B. and S. Leshner (1986). "Optical monitoring of membrane potential: methods of multisite optical measurement." Society of General Physiologists Series **40**(2): 71-99.
- Conti, E., N. P. Franks, et al. (1996). "Crystal structure of firefly luciferase throws light on a superfamily of adenylate-forming enzymes." Structure **4**(3): 287-98.
- Covarrubias, M., A. A. Wei, et al. (1991). "Shaker, Shal, Shab, and Shaw express independent K⁺ current systems." Neuron **7**(5): 763-73.
- Cramer, A., S. A. Raillard, et al. (1998). "DNA shuffling of a family of genes from diverse species accelerates directed evolution." Nature **391**(6664): 288-91.
- Cramer, A., E. A. Whitehorn, et al. (1996). "Improved green fluorescent protein by molecular evolution using DNA shuffling." Nature Biotechnology **14**(3): 315-9.
- Cubitt, A. B., R. Heim, et al. (1995). "Understanding, improving and using green fluorescent proteins." Trends in Biochemical Sciences **20**(11): 448-55.
- Cutler, M. W. and W. W. Ward (1993). Photochem. Photobiol. **57**(63s).
- Dascal, N., W. Schreibmayer, et al. (1993). "Atrial G protein-activated K⁺ channel: expression cloning and molecular properties." Proc Natl Acad Sci USA **90**: 10235-39.
- Dopf, J. and T. M. Horiagon (1996). "Deletion mapping of the *Aequorea victoria* green fluorescent protein." Gene **173**(1 Spec No): 39-44.
- Doupnik, C. A., N. Davidson, et al. (1995). "The inward rectifier potassium channel family." Current Biology **5**: 268-77.
- Drewe, J. A., S. Verma, et al. (1992). "Distinct spatial and temporal expression patterns of K⁺ channel mRNAs from different subfamilies." Journal of Neuroscience **12**(2): 538-48.
- González, J. E. and R. Y. Tsien (1997). "Improved indicators of cell membrane potential that use fluorescence resonance energy transfer." Chemistry and Biology **4**(4): 269-77.
- Gross, D. and L. M. Loew (1989). "Fluorescent indicators of membrane potential: microspectrofluorometry and imaging." Methods in Cell Biology **30**(1): 193-218.
- Gudermann, T., F. Kalkbrenner, et al. (1996). "Diversity and selectivity of receptor-g protein interaction." Annu. Rev. Pharmacol. Toxicol. **36**: 429-59.
- Haykin, S. S. (1994). Communication systems. New York, Wiley.

- Heim, R., A. B. Cubitt, et al. (1995). Nature **373**: 663-64.
- Heim, R. and R. Y. Tsien (1996). "Engineering green fluorescent protein for improved brightness, longer wavelengths and fluorescence resonance energy transfer." Current Biology **6**(2): 178-82.
- Hodgkin, A. L., A. F. Huxley, et al. (1952). "Measurements of current-voltage relations in the membrane of the giant axon of *Laligo*." J. Physiol (Lond) **116**: 424-48.
- Horton, R. M., H. D. Hunt, et al. (1989). "Engineering hybrid genes without the use of restriction enzymes: gene splicing by overlap extension." Gene **77**(1): 61-8.
- Hoshi, T., W. N. Zagotta, et al. (1990). "Biophysical and molecular mechanisms of Shaker potassium channel inactivation [see comments]." Science **250**(4980): 533-8.
- Hoshi, T., W. N. Zagotta, et al. (1991). "Two types of inactivation in Shaker K⁺ channels: effects of alterations in the carboxy-terminal region." Neuron **7**(4): 547-56.
- Isacoff, E. Y., Y. N. Jan, et al. (1990). "Evidence for the formation of heteromultimeric potassium channels in *Xenopus* oocytes [see comments]." Nature **345**(6275): 530-4.
- Isacoff, E. Y., Y. N. Jan, et al. (1991). "Putative receptor for the cytoplasmic inactivation gate in the Shaker K⁺ channel." Nature **353**(6339): 86-90.
- Johnson, F. H. and O. Shimomura (1978). Methods in Enzymology **57**: 271-291.
- Kamb, A., J. Tseng-Crank, et al. (1988). "Multiple products of the *Drosophila* Shaker gene may contribute to potassium channel diversity." Neuron **1**(5): 421-30.
- Katz, B. (1949). "Les constantes electriques de la membrane du muscle." Arch Sci Physiol **3**: 285-99.
- Kubo, Y., E. Reuveny, et al. (1993). "Primary structure and functional expression of a rat G protein-coupled muscarinic potassium channel." Nature **364**: 802-6.
- Levy, D. I. and C. Deutsch (1996). "A voltage-dependent role for K⁺ in recovery from C-type inactivation." Biophysical Journal **71**(6): 3157-66.
- Li, M., Y. N. Jan, et al. (1992). "Specification of subunit assembly by the hydrophilic amino-terminal domain of the Shaker potassium channel." Science **257**(5074): 1225-30.
- Loots, E. and E. Y. Isacoff (1998). "Protein rearrangements underlying slow inactivation of the Shaker K⁺ channel." Journal of General Physiology **112**(4): 377-89.

- Marshall, J., R. Molloy, et al. (1995). "The jellyfish green fluorescent protein: a new tool for studying ion channel expression and function." Neuron **14**(2): 211-5.
- Matz, M. V., A. F. Fradkov, et al. (1999). "Fluorescent proteins from nonbioluminescent Anthozoa species." Nature Biotechnology **17**(October): 969-73.
- McCormack, K., J. W. Lin, et al. (1990). "Shaker K⁺ channel subunits from heteromultimeric channels with novel functional properties." Biochemical and Biophysical Research Communications **171**(3): 1361-71.
- Miesenböck, G., D. A. De Angelis, et al. (1998). "Visualizing secretion and synaptic transmission with pH-sensitive green fluorescent proteins." Nature **394**(6689): 192-5.
- Miesenböck, G. and J. E. Rothman (1997). "Patterns of synaptic activity in neural networks recorded by light emission from synaptotagmins." Proceedings of the National Academy of Sciences of the United States of America **94**(7): 3402-7.
- Mitra, R. D., C. M. Silva, et al. (1996). "Fluorescence resonance energy transfer between blue-emitting and red-shifted excitation derivatives of the green fluorescent protein." Gene **173**(1 Spec No): 13-7.
- Miyawaki, A., O. Griesbeck, et al. (1999). "Dynamic and quantitative Ca²⁺ measurements using improved cameleons." Proceedings of the National Academy of Sciences of the United States of America **96**(5): 2135-40.
- Miyawaki, A., J. Llopis, et al. (1997). "Fluorescent indicators for Ca²⁺ based on green fluorescent proteins and calmodulin [see comments]." Nature **388**(6645): 882-7.
- Mostov, K., G. Apodaca, et al. (1992). "Plasma membrane protein sorting in polarized epithelial cells." Journal of Cell Biology **116**(3): 577-83.
- Neer, E. J. (1995). Cell **80**: 249-57.
- Nirenberg, S. and C. Cepko (1993). "Targeted ablation of diverse cell classes in the nervous system in vivo." Journal of Neuroscience **13**(8): 3238-51.
- Nobile, M., R. Olcese, et al. (1997). "Fast inactivation of Shaker K⁺ channels is highly temperature dependent." Experimental Brain Research **114**(1): 138-42.
- Olcese, R., R. Latorre, et al. (1997). "Correlation between charge movement and ionic current during slow inactivation in Shaker K⁺ channels." Journal of General Physiology **110**(5): 579-89.

- Ormö, M., A. B. Cubitt, et al. (1996). "Crystal structure of the *Aequorea victoria* green fluorescent protein [see comments]." Science **273**(5280): 1392-5.
- Palm, G. J., A. Zdanov, et al. (1997). "The structural basis for spectral variations in green fluorescent protein." Nature Structural Biology **4**(5): 361-65.
- Perozo, E., L. Santacruz-Toloza, et al. (1994). "S4 mutations alter gating currents of Shaker K channels." Biophysical Journal **66**(2 Pt 1): 345-54.
- Prasher, D. C., V. K. Eckenrode, et al. (1992). "Primary structure of the *Aequorea victoria* green-fluorescent protein." Gene **111**(2): 229-33.
- Rizzuto, R., M. Brini, et al. (1996). "Double labelling of subcellular structures with organelle-targeted GFP mutants in vivo." Current Biology **6**(2): 183-8.
- Rizzuto, R., A. W. Simpson, et al. (1992). "Rapid changes of mitochondrial Ca²⁺ revealed by specifically targeted recombinant aequorin [published erratum appears in Nature 1992 Dec 24-31;360(6406):768]." Nature **358**(6384): 325-7.
- Romoser, V. A., P. M. Hinkle, et al. (1997). "Detection in living cells of Ca²⁺-dependent changes in the fluorescence emission of an indicator composed of two green fluorescent protein variants linked by a calmodulin-binding sequence. A new class of fluorescent indicators." Journal of Biological Chemistry **272**(20): 13270-4.
- Roska, B., E. Nemeth, et al. (1998). "Response to change is facilitated by a three-neuron disinhibitory pathway in the tiger salamander retina." Journal of Neuroscience **18**(9): 3451-9.
- Roush, W. (1996). Science **271**: 1056-58.
- Ruppersberg, J. P., K. H. Schröter, et al. (1990). "Heteromultimeric channels formed by rat brain potassium-channel proteins [see comments]." Nature **345**(6275): 535-7.
- Sambrook, J., E. F. Fritsch, et al. (1989). Molecular cloning : a laboratory manual. Cold Spring Harbor, N.Y., Cold Spring Harbor Laboratory.
- Shen, N. V., X. Chen, et al. (1993). "Deletion analysis of K⁺ channel assembly." Neuron **11**(1): 67-76.
- Shojiro, I., C. Kondo, et al. (1997). "Inwardly rectifying potassium channels: their molecular heterogeneity and function." Japanese Journal of Physiology **47**: 11-39.

- Siegel, M. S. and E. Y. Isacoff (1997). "A genetically encoded optical probe of membrane voltage." Neuron **19**(4): 735-41.
- Simering, K. R., R. Golbik, et al. (1996). "Mutations that suppress the thermosensitivity of green fluorescent protein." Current Biology **6**(12): 1653-63.
- Stadel, J. M., S. Wilson, et al. (1997). "Orphan G protein-coupled receptors: a neglected opportunity for pioneer drug discovery." Trends in Pharmaceutical Sciences **18**: 430-37.
- Stryer, L. (1978). "Fluorescence energy transfer as a spectroscopic ruler." Annual Review of Biochemistry **47**(1): 819-46.
- Stühmer, W., J. P. Ruppersberg, et al. (1989). "Molecular basis of functional diversity of voltage-gated potassium channels in mammalian brain." Embo Journal **8**(11): 3235-44.
- Tempel, B. L., D. M. Papazian, et al. (1987). "Sequence of a probable potassium channel component encoded at Shaker locus of Drosophila." Science **237**(4816): 770-5.
- Timpe, L. C., Y. N. Jan, et al. (1988). "Four cDNA clones from the Shaker locus of Drosophila induce kinetically distinct A-type potassium currents in Xenopus oocytes." Neuron **1**(8): 659-67.
- Tsien, R. Y. (1989). "Fluorescent probes of cell signaling." Annual Review of Neuroscience **12**(1): 227-53.
- Tsien, R. Y. (1998). "The green fluorescent protein." Annual Review of Biochemistry **67**(5347): 509-44.
- Tsien, R. Y. (1999). "Rosy dawn for fluorescent proteins." Nature Biotechnology **17**(October): 956-57.
- Ward, W. H., H. J. Prentice, et al. (1982). "Spectral perturbations of the Aequorea green-fluorescent protein." Photochem. Photobiol. **35**: 803-808.
- Warrens, A. N., M. D. Jones, et al. (1997). "Splicing by overlap extension by PCR using asymmetric amplification: an improved technique for the generation of hybrid proteins of immunological interest." Gene **186**(1): 29-35.
- Yang, F., L. G. Moss, et al. (1996). "The molecular structure of green fluorescent protein." Nature Biotechnology **14**(10): 1246-51.
- Zagotta, W. N., T. Hoshi, et al. (1990). "Restoration of inactivation in mutants of Shaker potassium channels by a peptide derived from ShB [see comments]." Science **250**(4980): 568-71.
- Zito, K., R. D. Fetter, et al. (1997). "Synaptic clustering of Fascilin II and Shaker: essential targeting sequences and role of Dlg." Neuron **19**(5): 1007-16.

Zolotukhin, S., M. Potter, et al. (1996). "A "humanized" green fluorescent protein cDNA adapted for high levels of expression in mammalian cells." Journal of Virology 70: 4646-54.

"You cannot say, or guess, for you know only
A heap of broken images, where the sun
beats..."

-T.S. Eliot (1922)